Supporting Information for

Biliatresone, A Reactive Natural Toxin from *Dysphania glomulifera* and *D. littoralis*: Discovery of the Toxic Moiety 1,2-Diaryl-2-Propenone

Kyung A. Koo,[*,†] Kristin Lorent,[‡] Weilong Gong,[‡] Peter Windsor,[⊥] Stephen J. Whittaker,[#] Michael Pack,[‡,∥] Rebecca G. Wells,[‡,§] and John R. Porter[*,†]

[†]Department of Biological Sciences, University of the Sciences, Philadelphia, Pennsylvania 19104, USA

[‡]Departments of Medicine, [∥]Cell Biology, [§]Pathology and Laboratory Medicine, Perelman School of Medicine, University of Pennsylvania, Philadelphia 19104, USA

[⊥]Faculty of Veterinary Science, University of Sydney, Sydney, New South Wales 2006, Australia

[#]Hume Livestock and Pest Authority, Albury Area, New South Wales, Australia

*To whom correspondence should be addressed.
E-mail: j.porter@usciences.edu and k.koo@usciences.edu

Contents

Supplementary Data

Abbreviations:

ACN	Acetonitrile
ASAP	Atmospheric Solids Analysis Probe
CD	Circular Dichroism
COSY	Correlation Spectroscopy
DAD	Diode Array Detector
DEPT	Distortionless Enhancement by Polarization Transfer
DMSO	Dimethyl Sulfoxide
dpf	Days Post-Fertilization
ESI	Electro Spray Ionization
EtOAc	Ethyl Acetate
EtOH	Ethanol
FT-IR	Fourier Transform Infrared
Fr	Fraction
Hex	Hexane
HMBC	Heteronuclear Multiple Bond Correlation
HMQC	Heteronuclear Multiple Quantum Correlation
HPLC	High Performance Liquid Chromatography
HRMS	High Resolution Mass Spectrometry
HSQC	Heteronuclear Single Quantum Coherence
LC-MS	Liquid Chromatography-Mass Spectrometry
MeOH	Methanol
MS	Mass Spectrometry
NMR	Nuclear Magnetic Resonance
ODS	Octadecyl-Silica
Pet	Petroleum
RP-HPLC	Reverse Phase-High Performance Liquid Chromatography
Subfr	Sub-fraction
t_R	Retention Time
UV	Ultraviolet

General Experimental Procedures

HPLC-grade solvents (petroleum ether, hexane, CH_2Cl_2, EtOAc, EtOH, MeOH, ACN, and water) were purchased from Sigma-Aldrich (St. Louis, MO, USA) and used in all processes, including RP-HPLC and LC-MS. Synthesis reagents (1,2-diaryl-ethanone, piperidine, acetic acid, formalin (37%), and $NaHCO_3$) were purchased from Sigma-Aldrich (St. Louis, MO, USA). RP-HPLC was performed at room temperature in an Agilent 1100 series system (Santa Clara, CA, USA) equipped with vacuum degasser, quaternary pump, thermostatically-controlled column compartment, and DAD. LC-MS (ESI, positive mode, *m/z*) spectra were collected on a Shimadzu LCMS-2010EV system (Kyoto, Japan) with UV detector.

The chemical structures were elucidated by the analytical spectroscopic techniques of FT-IR, CD, HRMS, ^{1}H NMR, ^{13}C NMR, DEPT135, and 2D NMR techniques (^{1}H-^{1}H COSY, HMQC, HSQC, NOESY, and HMBC). FT-IR was recorded as a thin film on a ZnSe plate with a Nicolet Avatar 370DTGS spectrometer (Thermo Electron Corporation). CD spectra were measured at 25°C and a speed of 1 nm·s^{-1} as a thin film in a demountable rectangular cell with path length of 0.5 mm in an AVIV model 410 spectrometer (AVIV Biomedical, Inc. Lakewood, NJ, USA) equipped with a temperature controller. To obtain HRMS, ASAP (ESI, positive mode) was operated in a Thermo Scientific Exactive spectrometer powered by Orbitrap technology. The differences (*ppm*) value between a found (*F*) and a calculated value (*C*) were calculated from the equation *ppm* Difference = $|F\text{-}C|/C \times 10^6$. The NMR spectra were acquired on a Bruker AVANCE 400 or 400II spectrometer with ^{1}H and ^{13}C frequencies of 400 and 100 MHz, respectively. Chemical shifts were in *ppm* and relative to tetramethylsilane; coupling constants (*J*) were reported in *Hz*. The NMR lock solvents (acetone-d_6 and CD_3OD) were purchased from Cambridge Isotope Laboratories.

Plant Materials

A sample (~2.8 kg) containing a mixture of *D. glomulifera* and *D. littoralis* were collected from the area

of the Murray river, along the Hume Weir, near Albury, NSW, Australia (latitude -36.003°, longitude 147.139°) by S.J. Whittaker; the plants were collected from the flats exposed by the drop of the reservoir level during extreme drought. The plants were identified by Surrey Jacobs (Royal Botanic Gardens, Melbourne, Australia). Voucher specimens for the population are housed at the National Herbarium of Victoria (MEL). The plants were frozen until shipment (-18°C), and shipped on dry ice to the authors' laboratories in April 2009 under a plant import permit from Animal Plant Health and Inspection Service, US Department of Agriculture (permit no. P37-08-00668, 21 May 2008). Individual plants were carefully teased from the frozen biomass and preserved as voucher specimens deposited in the herbarium of the University of the Sciences in Philadelphia (PHIL).

Extraction, Fractionation, and Isolation

Freeze-dried plants (100 g) were ground to pass a 20 mesh screen and extracted at room temperature in a blender with 1:1 (v/v) CH_2Cl_2/MeOH. As shown in figure S2A, the plant material residue was removed by filtration and extracted twice more in the same solvent to give the CH_2Cl_2/MeOH extract. The plant material residue was extracted with water (×3), and the aqueous extracts were pooled as a water extract. After partial evaporation *in vacuo* to about half of the original volume, water was added to the CH_2Cl_2/MeOH organic extract and then partitioned with petroleum ether (bp 40-60°C); the pet. ether fractions were pooled. All fractions were evaporated to dryness *in vacuo* (organic) or by lyophilization (aqueous) and subjected to bioassay.

The CH_2Cl_2/MeOH extract (Fr1) was subjected to diol silica gel flash column chromatography with hexane, CH_2Cl_2, EtOAc, MeOH, and water to generate five solvent fractions partitioned by polarity. The active CH_2Cl_2 fraction was further separated to seven subfractions through RP-HPLC on a semi-preparative Phenomenex ultracarb 10 ODS-20 (600×10 mm, 10 μm, 5 $mL \cdot min^{-1}$) column in a linear gradient elution of water to MeOH (5 → 95 % MeOH) with DAD detection at 206 and 254 nm. The seven subfractions were taken to dryness *in vacuo* and by lyophilization and submitted to bioassay. The two active subfractions (subFr45) were further purified by semi-preparative RP-HPLC on a YMC

J'sphere ODS-H80 (250×10 mm, 4 μm, 3 mL·min^{-1}) column in an isocratic solvent system of water/MeOH/ACN (4:3:3, v/v/v) and yielded four compounds (**1**-**4**). The toxic fractions, subfractions, and individual compounds were analyzed in the RP-HPLC and LC-MS (ESI, positive mode, *m/z*) with a Waters Symmetry C18 column (250×4.6 mm, 5 μm, 0.2, 0.3 or 0.5 mL·min^{-1}) in the mobile phase of water/MeOH/ACN (4:3:3, v/v/v), water/EtOH/ACN (4:3:3, v/v/v) or water/ACN (1:1, v/v) with UV detection. The toxicity of the six compounds (**1**-**4**) on the zebrafish larvae was assayed; we confirmed that **1** caused significant biliary dysfunction. The dry weight of the plant material was 6.08% of the frozen weight of the plant; other yield data can be found in figure S2B. The yield of toxic compound **1** was collectively approximately 1.84% of the dry weight of the plant.

Solvent adducts (**1w** and **1m**) and biliatresone (**1**) were purified in the EtOH-based solvent to remove the interference of MeOH and dried directly *in vacuo*. RP-HPLC and LC-MS analysis of the purified compounds were performed with a Waters Symmetry C18 column (250×4.6 mm, 5 μm, 0.3 mL·min^{-1}) in a mixture of water/EtOH/ACN (4:3:3:, v/v/v). For compound **1d**, the tiny peak at t_R 22.18 min or t_R 22.69 was purified by RP-HPLC with a Waters Symmetry C18 column (250×4.6 mm, 5 μm, 0.5 mL·min^{-1}) in a mixture of water/ACN (1:1, v/v), which leads to higher difference of retention time between **1** and **1d**. This collection was evaporated directly to dryness *in vacuo*. ^{1}H NMR and HMBC data were acquired in acetone-d_6 lock solvent.

Chemical Structure Elucidations

Compound **1** was isolated as a yellowish gum. The ^{13}C NMR spectrum (Figure S4 and Table S1) showed 18 carbons including a carbonyl group (δ_C=195.7 ppm, C1′). The DEPT135 spectrum showed two peaks corresponding to dioxymethylene (δ_C=102.5 ppm, C1a) and methylene (δ_C=130.1 ppm, C3') carbons. Among the 16 protons in the ^{1}H NMR spectrum, a broad proton peak (δ_H=8.05 ppm, OH) was not correlated to a carbon in the HMQC spectrum (Figure S5). This proton showed a correlation to the phenyl carbons (δ_C=116.9 ppm, C3" and δ_C=125.9 ppm, C1") in the HMBC spectrum (Figure S6). An olefinic protons (δ_H=6.04, 6.08 ppm, 3'-H) was typical of a α-methylene with no splitting; these were

correlated with the carbonyl carbon (δ_C=195.7 ppm, C1') and a quaternary aromatic carbon (δ_C=125.9 ppm, C1") in the HMBC. The HMBC spectrum showed correlations from 1a-H to C1 and C2; 3-H to C1, C2, C4 and C5; 3′-H to C1′, C2′ and C1"; 3"-H to C2" and C5"; 4"-H to C2" and C6"; 5"-H to C1" and C3"; 6"-H to C2′, C2" and C4" (Figure S6). The NOESY spectrum presented only a cross-peak correlation between 3-H and 4-methoxyl proton (-OCH_3) (Figure S7).

Biliatresone (**1**): yellowish gum; CD (deg, film): $\Delta\varepsilon$ = −0.3 (240 nm), $\Delta\varepsilon$ = +0.5 (290 nm); ^{1}H NMR and ^{13}C NMR, see Table 1; IR (film): λ_{max} 3379, 2925, 1622, 1485, 1202, 1074, 932, 751 cm^{-1}; HPLC-UV/vis (aq MeOH and ACN): λ_{max} 235, 281 nm; HR-ASAP-MS (ESI, positive mode, *m/z*): 329.1022 $[M+H]^+$ calcd for $C_{18}H_{17}O_6$, 329.1025. Values of ^{1}H NMR spectroscopy of biliatresone (**1**) measured in the CD_3OD lock solvent were acquired from biliatresone newly purified in an EtOH-based solvent to compare with values of the ^{1}H NMR of a mixture of **1** and **1m** in the CD_3OD lock solvent. ^{1}H NMR (400MHz, CD_3OD, *ppm*): δ_H 7.13 (m, 2H), 6.81 (m, 2H), 6.39 (s, 1H), 6.07 (s, 1H), 6.01 (s, 1H), 5.94 (s, 2H), 3.95 (s, 3H), 3.70 (s, 3H).

Compound **2** was isolated as a white powder. The HRMS showed a molecular mass of *m/z* 313.0708 $[M+H]^+$ (calculated for $C_{17}H_{13}O_6$, 313.0712), indicating a molecular formula of $C_{17}H_{12}O_6$. By comparing our NMR data with the literature (Figures S9-S10), **2** was identified as betavulgarin, 2′-hydroxy-6,7-methylenedioxy-5-methoxyisoflavone.[1]

Betavulgarin (**2**): White powder; ^{1}H NMR (400 MHz, acetone-d_6, *ppm*): δ_H 4.01 (s, 3H), 6.24 (s, 2H), 6.93 (s, 1H), 6.96 (m, 2H), 7.29 (m, 2H), 8.23 (s, 1H), 9.04 (s, OH); HPLC-UV/vis (aq MeOH and ACN): λ_{max} 218, 246, 324 nm; LC-MS (ESI, positive mode, *m/z*): 313 $[M+H]^+$, 376 $[M+Cu]^+$; HR-ASAP-MS (ESI, positive mode, *m/z*): 313.0708 $[M+H]^+$ calcd for $C_{17}H_{13}O_6$, 313.0712.

Compound **3** was isolated as a yellowish gum. LC-MS analysis gave a mass of *m/z* 315 $[M+H]^+$ indicating a molecular formula of $C_{17}H_{14}O_6$; this was confirmed by the HR-MS analysis (*m/z* 315.0864 $[M+H]^+$; calculated for $C_{17}H_{15}O_6$, 315.0869) (Figures S11 and S16). UV spectrum and a three proton spin system, 3-H (δ_H=4.11 ppm), 2α-H (δ_H=4.51 ppm), and 2β-H (δ_H=4.66 ppm), of the ^{1}H NMR data were typical of an isoflavanone skeleton (Figures S11 and S12). Seventeen carbons in the ^{13}C NMR and DEPT135 spectra, including the dioxymethylene carbon (δ_C=102.9 ppm, C6a), the methoxyl carbon (δ_C=60.8 ppm) and the methylene carbon (δ_C=71.0 ppm, C2), were also typical of an isoflavonoid (Figure S13). The hydroxy proton (δ_H=8.73 ppm, OH) showed correlations with the C1′ and C2′ carbons of the B ring in the HMBC spectrum (Figure S15). From 1D and 2D analysis (Table S2) along with the CD analysis suggested that **3** has the *S*-stereoisomer configuration, with a negative Cotton effect between 290 and 340 nm, corresponding to a n→π* transition energy (Figure S17), we identified the chemical structure of **3** as (3*S*) 2′-hydroxy-5-methoxy-6,7-methylenedioxy isoflavanone, not previously reported.

(3*S*) 2′-Hydroxy-5-methoxy-6,7-methylenedioxyisoflavanone (**3**): Yellowish gum; CD (deg, film): Δε = 1.5 (180 nm), Δε = −1.2 (244 nm), Δε = −0.27 (310 nm); ^{1}H NMR and ^{13}C NMR, see Table 2; IR (film): ν_{max} 3575, 2918, 2850, 1625, 1475, 1250, 1100, 930, 776 cm^{-1}; HPLC-UV/vis (aq MeOH and ACN): λ_{max} 245, 283, 342 nm; LC-MS (ESI, positive mode, *m/z*): 315 $[M+H]^+$, 378 $[M+Cu]^+$; HR-ASAP-MS (ESI, positive mode, *m/z*): 315.0864 $[M+H]^+$ calcd for $C_{17}H_{15}O_6$, 315.0869.

Compound **4** was isolated as a yellowish gum and purified by RP-HPLC (Table S2). The LC-MS analysis showed a major peak at *m/z* 329 $[M+H]^+$, leading to a molecular formula of $C_{18}H_{16}O_6$, verified by the mass at *m/z* 328.0945 $[M]^+$ (calculated for $C_{18}H_{16}O_6$, 328.0947) in the HR-MS data (Figures S18 and S22). The ^{1}H NMR spectrum displayed resonances for two aromatic ring protons in a di-substituted phenyl moiety (δ_H=7.2-7.8 ppm, 4′-H, 5′-H, 6′-H, 7′-H) and a phenyl moiety with the dioxymethylene group at (δ_H=6.03 ppm, 1a-H), together with a methine proton (δ_H=6.54 ppm, 3-H) and two methoxyl protons

(δ_H=3.72, 3.89 ppm) (Figure S19). The ^{13}C NMR and HMQC spectra exhibited resonances for 18 carbons, including the dioxymethylene carbon (δ_C=102.5 ppm, C1a), two methoxyl carbons (δ_C=60.4, 57.0 ppm), a methine carbon (δ_C=90.1 ppm, C3), and a primary alcohol (δ_C=56.4 ppm) (Figures S19 and S20). In the HMBC spectrum, the methine proton (δ_H=6.54 ppm, 3-H) showed correlations to the dioxymethylene carbons, C1 and C2 (δ_C=131.6, 152.2 ppm), C4 (δ_C=155.9 ppm), and C5 (δ_C=104.9 ppm) (Figure S21). The primary alcohol proton (δ_H=4.58 ppm) showed correlations with three carbons, C3′ (δ_C=119.9 ppm), C2′ (δc=147.5 ppm) and C3′a (δ_C=130.0 ppm), in the di-substituted phenyl ring. From 1D and 2D analysis (Table S2), the structure of **4** was identified as a novel seco-pterocarpan, 1,2-methylenedioxy-4-methoxy-seco-pterocarpan. We have given **4** the trivial name of 'humeone' in recognition of plant collection along the Hume Weir.

1,2-Methylenedioxy-4-methoxy-seco-pterocarpan (**4**): Yellowish gum; CD (deg, film): Δε = −3.6 (195 nm), Δε = +0.2 (300 nm); ^{1}H NMR and ^{13}C NMR, see Table 2; IR (film) ν_{max} 2912, 2843, 1468, 1440, 1202, 1074, 932, 739 cm^{-1}; HPLC-UV/vis (aq MeOH and ACN): λ_{max} 245, 294 nm; LC-MS (ESI, positive mode, *m/z*): 311 $[M-H_2O]^+$, 329 $[M+H]^+$; HR-ASAP-MS (ESI, positive mode, *m/z*): 328.0945 $[M]^+$ calcd for $C_{18}H_{16}O_6$, 328. 0947.

3′-Methoxy-biliatresone (**1m**): yellowish gum; ^{1}H NMR and ^{13}C NMR, see Table 1; HPLC-UV/vis (aq MeOH and ACN): λ_{max} 281, 310 nm; HRMS (ESI, positive mode, *m/z*): 361.1270 $[M+H]^+$ calcd for $C_{19}H_{20}HO_7$, 361.1287; LC-MS (ESI, positive mode, *m/z*): 361 $[M+H]^+$ (calcd for $C_{19}H_{21}O_7$), and 383 $[M+Na]^+$ (calcd for $C_{19}H_{20}NaO_7$).

Demethylene biliatresone (**1d**): ^{1}H NMR (400MHz, acetone-d_6; *ppm*): δ_H 7.11 (t, *J*=8, 1H), 7.06 (d, *J*=7.6, 1H), 6.84 (d, *J*=8, 1H), 6.77 (t, *J*=7.6, 1H), 6.43 (s, 1H), 5.97 (s, 2H), 4.03 (s, 2H), 3.86 (s, 3H), 3.76 (s, 3H); HPLC-UV/vis (aq MeOH and ACN): λ_{max} 285, 267 nm; LC-MS (ESI, positive mode, *m/z*): 317

$[M+H]^+$ (calculated for $C_{17}H_{17}O_6$, 317.103).

Synthesis of 1,2-diaryl-2-propen-1-one (5)

The 1,2-diaryl-ethanone (5 g, 25.5mmol) in MeOH (45 mL) was treated with piperidine (0.2 mL), acetic acid (0.2 mL) and 37% formalin (5.4 mL). The mixture was refluxed for 3 h at 95-100^{o}C. After cooling, ice-cold 3% $NaHCO_3$ was gradually added into the reaction mixture to pH 7.4 (approx. 150mL). The reactant was put in the refrigerator for 18 h to precipitate the semi-solid product. Supernatant was removed and then added water and CH_2Cl_2 to liquid-liquid extraction. The CH_2Cl_2 fraction containing the product was collected and dried. It was a colorless oil (94% yield).[2]

1,2-Diaryl-2-propen-1-one (**5**): colorless oil; ^{1}H NMR (400MHz, acetone-d_6, *ppm*): δ_H 7.99 (d, *J*=8.2, 2H), 7.52 (dd *J*=7.4, 4H), 7.38 (m, 4H), 6.15 (s, 1H), 5.63 (s, 1H); ^{13}C NMR (100 MHz, acetone-d_6, *ppm*): δ_C 196.9, 148.3, 137.3, 137.2, 133.2, 129.8, 128.8 128.7, 127.1, 120.4; LC-MS (ESI, positive mode, *m/z*): 209 $[M+H]^+$ (calcd for $C_{15}H_{13}O$) and 231 $[M+Na]^+$ (calcd for $C_{15}H_{12}NaO$).

Zebrafish Toxicity Assay

Plant extracts, fractions and compounds were suspended in anhydrous DMSO to give stock samples. Zebrafish larvae reared in 24- and 96-well plates were exposed to the sample for 24-72 h (final concentration 1% DMSO in the medium) with various concentrations. For the initial extract and fractions, concentrations of 5-50 μg/ml were tested. The final compounds were tested at 0.0625-1.0 μg/ml. The embryo medium with extract was exchanged daily. Following treatment of the zebrafish larva, the fluorescent long chain fatty acid Bodipy-C16 (Invitrogen) was added to the water as previously described.[3] Gallbladder and intestinal fluorescence in the treated and control larva were examined with a stereomicroscope (Olympus MVX-10). All assays were performed in triplicate and controls for swallowing were performed with each sample.

References

(1) Elliger, C. A. and Halloin, J. M. (1994) Phenolics induced in *Beta vulgaris* by *Rhizoctonia solani* infection. *Phytochemistry 37*, 691–693.

(2) Tramontini, M. (1973) Advances in the chemistry of Mannich bases. *Synthesis 12*, 703–775.

(3) Lorent, K., Moore, J. C., Siekmann, A. F., Lawson, N., and Pack, M. (2010) Reiterative use of the notch signal during zebrafish intrahepatic biliary development. *Dev. Dynam. 239*, 855–864.

Supplementary Data

A.

B.

Figure S1. The toxic plants *Dysphania glomulifera* and *D. littoralis*. (A) We collected the plants from the pasture associated with the 2007 outbreak. The Murray River reservoir impounded by the Hume Dam (formerly the Hume Weir) is visible in the background. (B) A grouping of the plants at the collection site. *D. glomulifera* and *D. littoralis* often grow together and can be differentiated only microscopically. Images courtesy of author Steven J. Whittaker, 2007.

A.

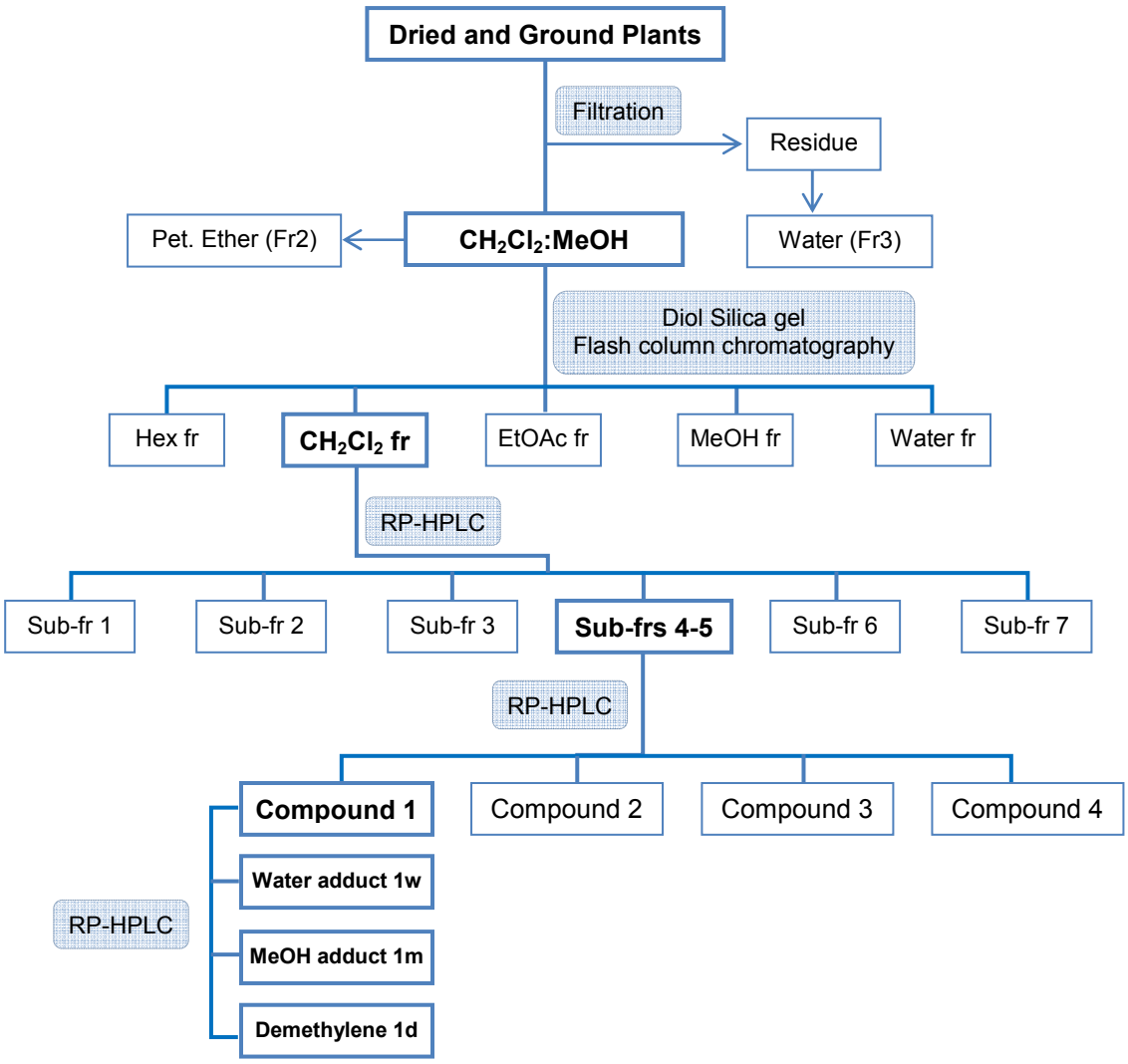

B.

Toxic components	% of dry weight
Dry weight	100.00
CH_2Cl_2:MeOH extract	40.05
CH_2Cl_2 fraction (Fr1)	8.53
Subfractions 4 and 5 (subFr45)	4.08
1 and its derivatives (**1w**, **1m**, and **1d**)	1.84

Figure S2. The isolation scheme of compounds (**1**-**4**) (A) and yield of the toxic components (B). The bolded fractions and compounds showed toxicity in the zebrafish assay.

A.

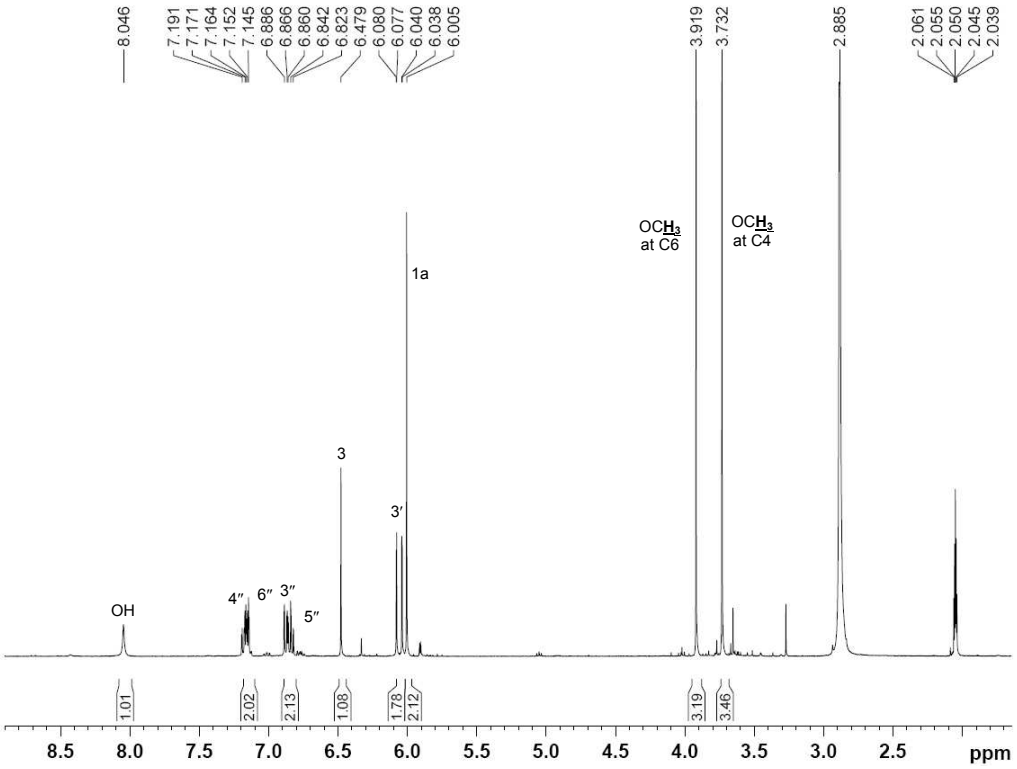

B.

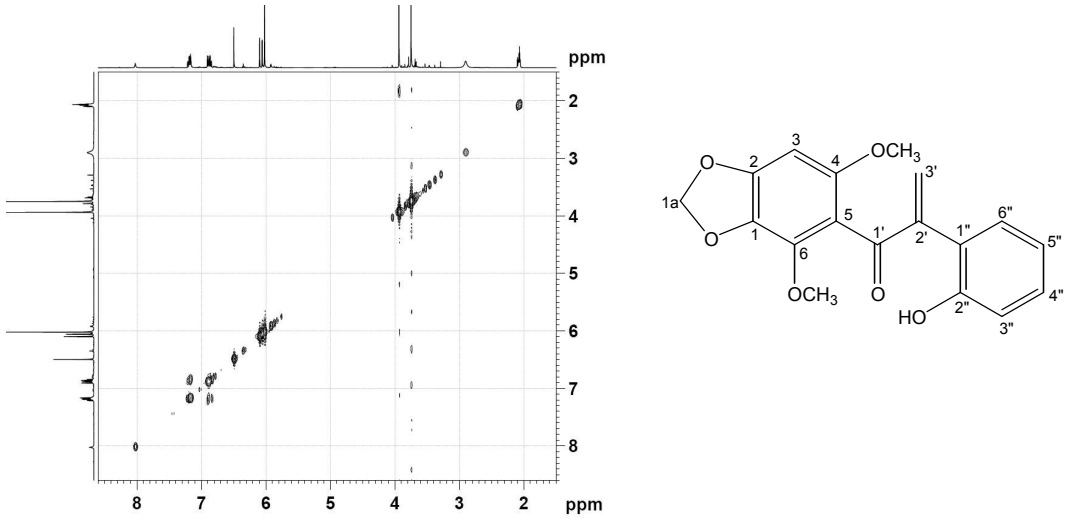

Figure S3. ^{1}H NMR spectrum (A) and ^{1}H-^{1}H COSY spectrum (B) for **1** (400 MHz, acetone-d_6).

A.

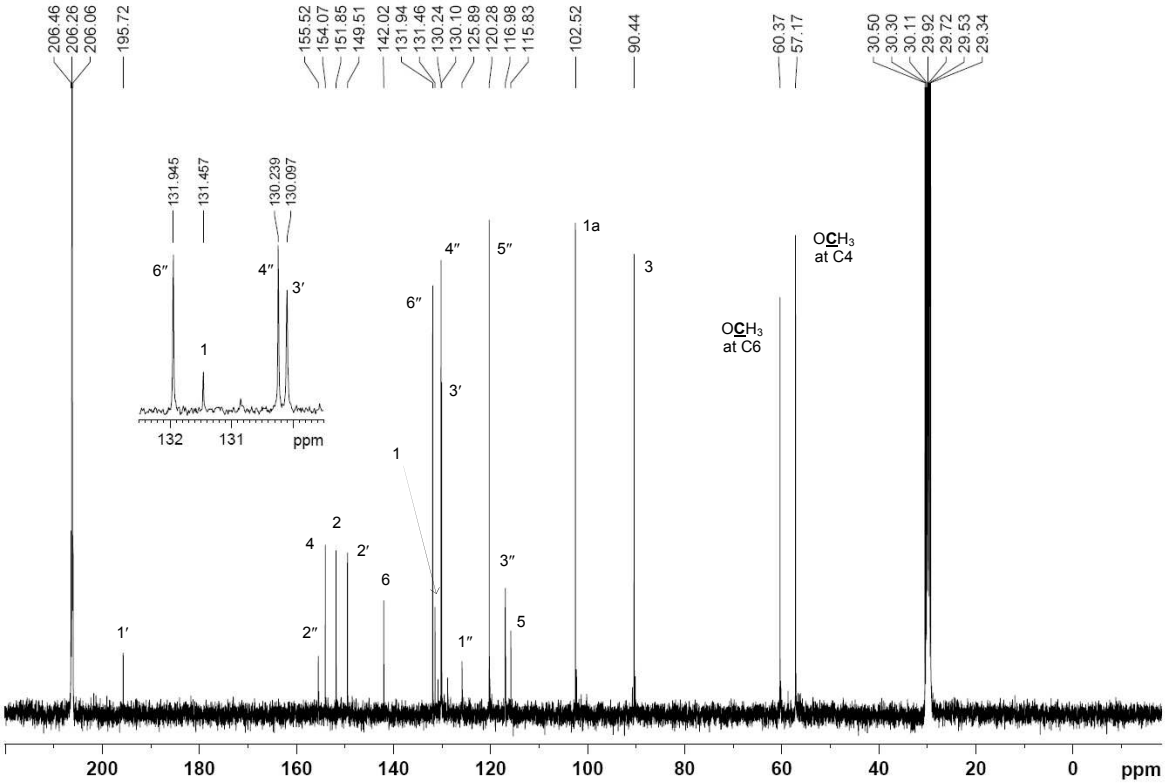

B.

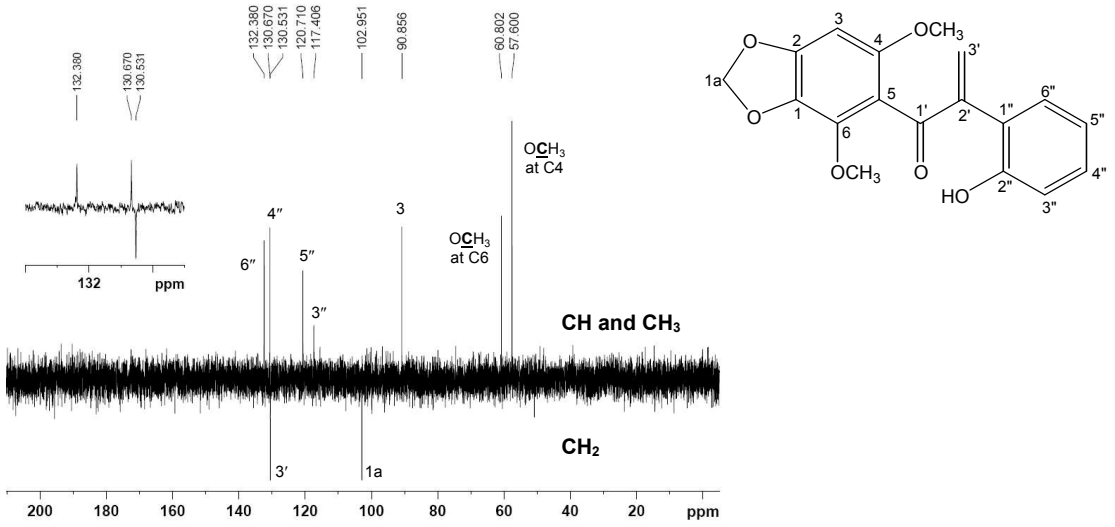

Figure S4. ^{13}C NMR spectrum (A) and DEPT 135 spectrum (B) for **1** (100 MHz, acetone-d_6).

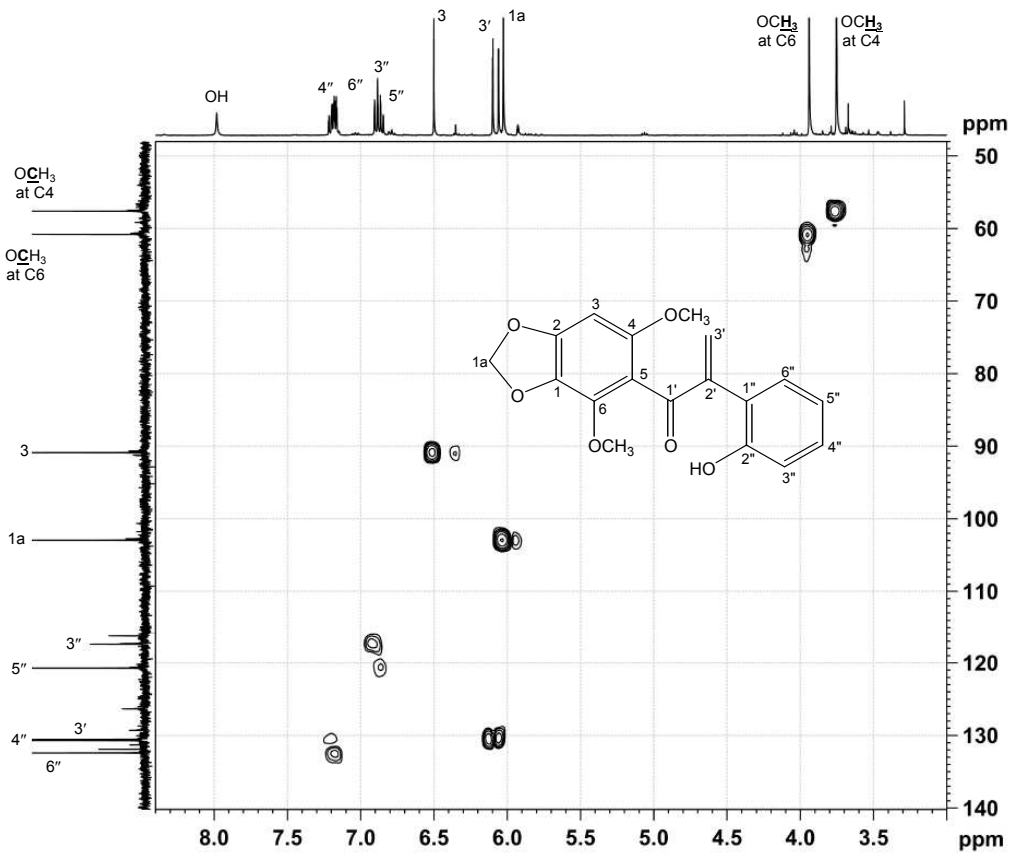

Figure S5. HMQC spectrum for **1** (100 MHz, acetone-d_6).

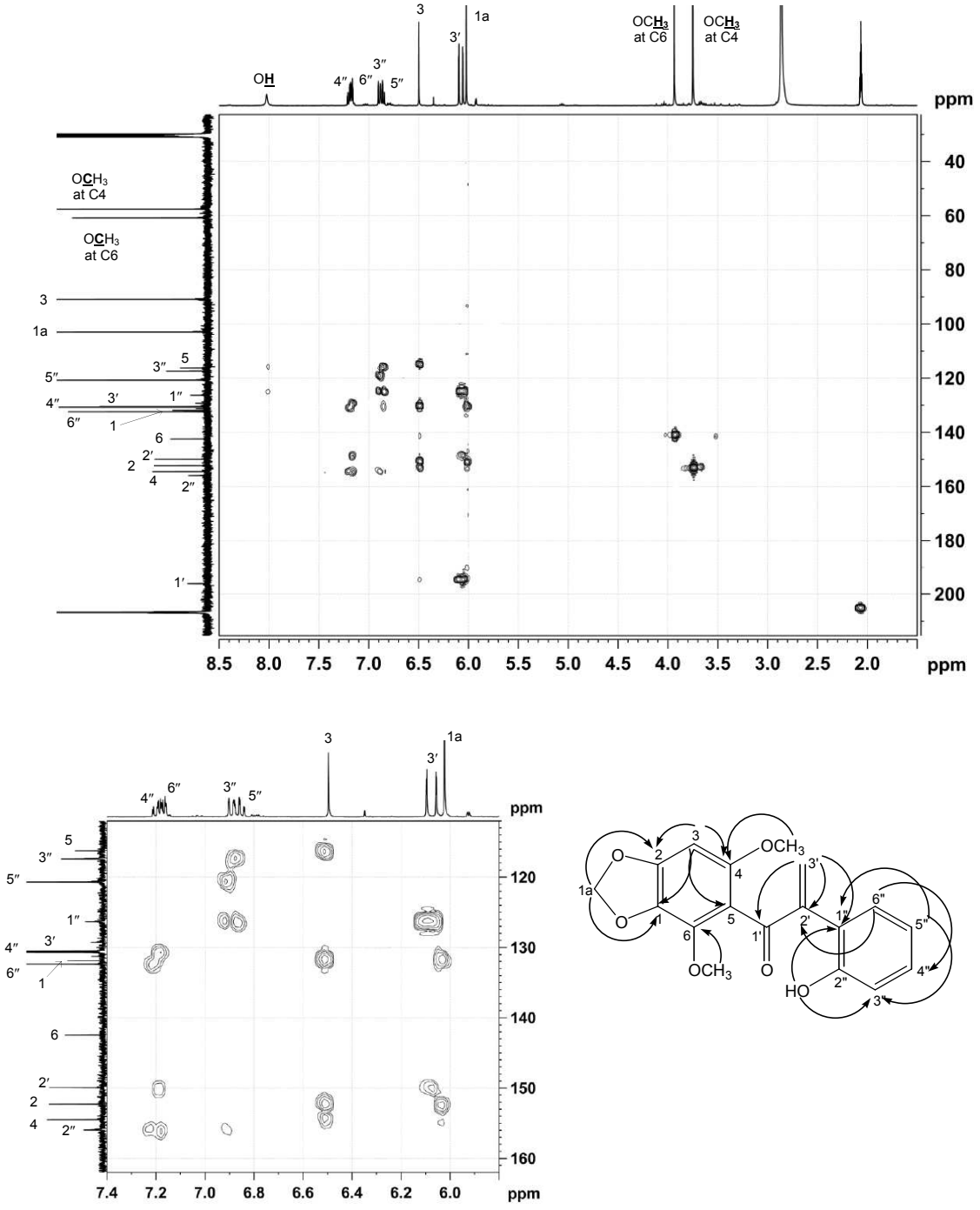

Figure S6. HMBC spectrum for **1** (100 MHz, acetone-d_6). Major interactions are indicated in the compound structure.

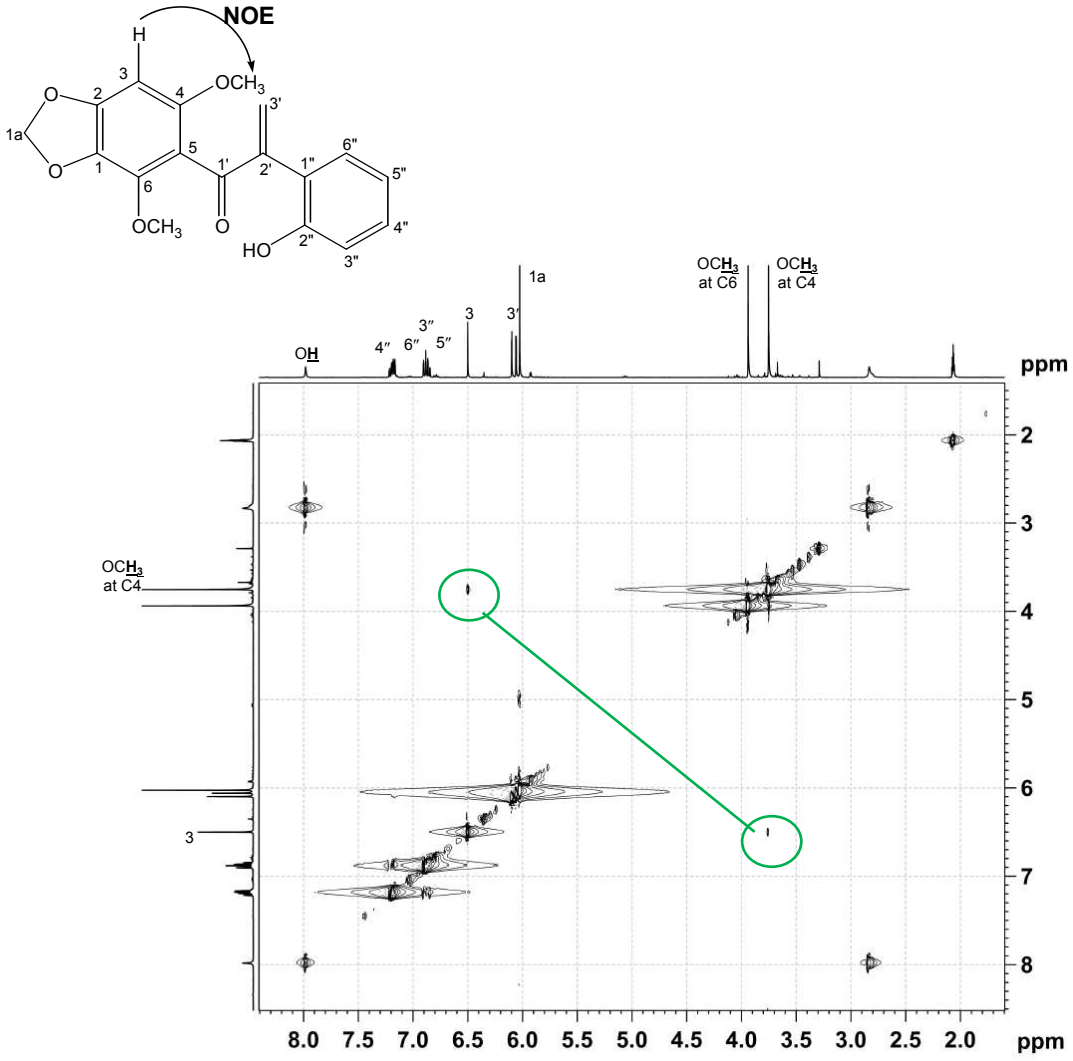

Figure S7. NOESY spectrum for **1** (400 MHz, acetone-d_6). The major NOE interaction is shown by the green line connecting the circled resonances (H→H NOE).

A.

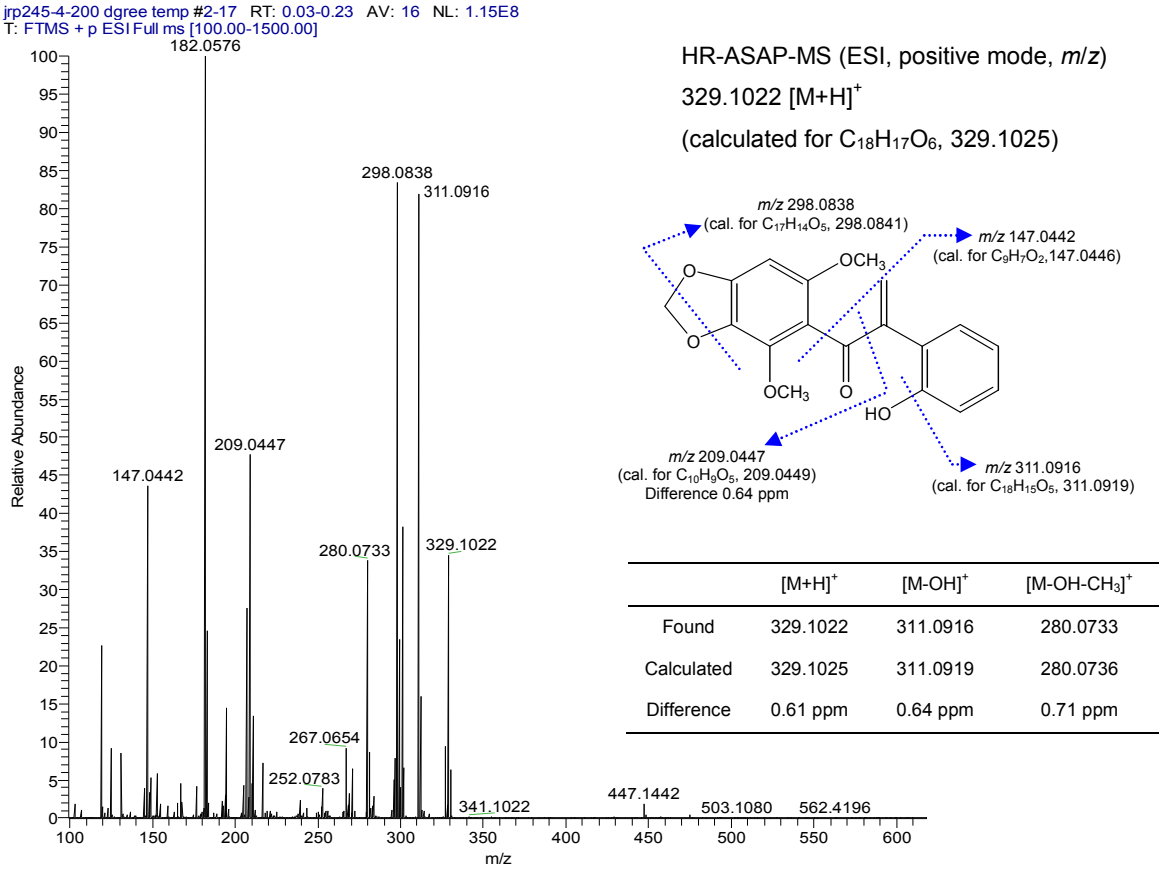

	$[M+H]^+$	$[M-OH]^+$	$[M-OH-CH_3]^+$
Found	329.1022	311.0916	280.0733
Calculated	329.1025	311.0919	280.0736
Difference	0.61 ppm	0.64 ppm	0.71 ppm

B.

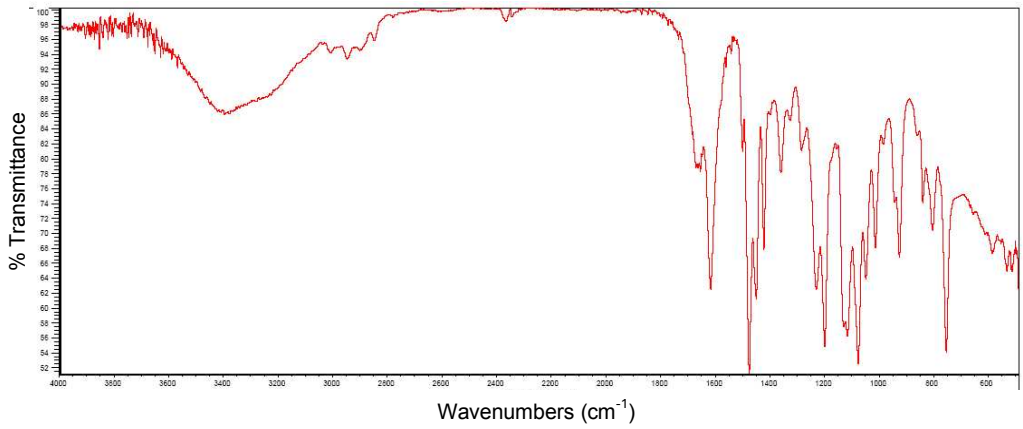

Figure S8. HRMS spectrum (A) and FT-IR spectrum (B) for **1**.

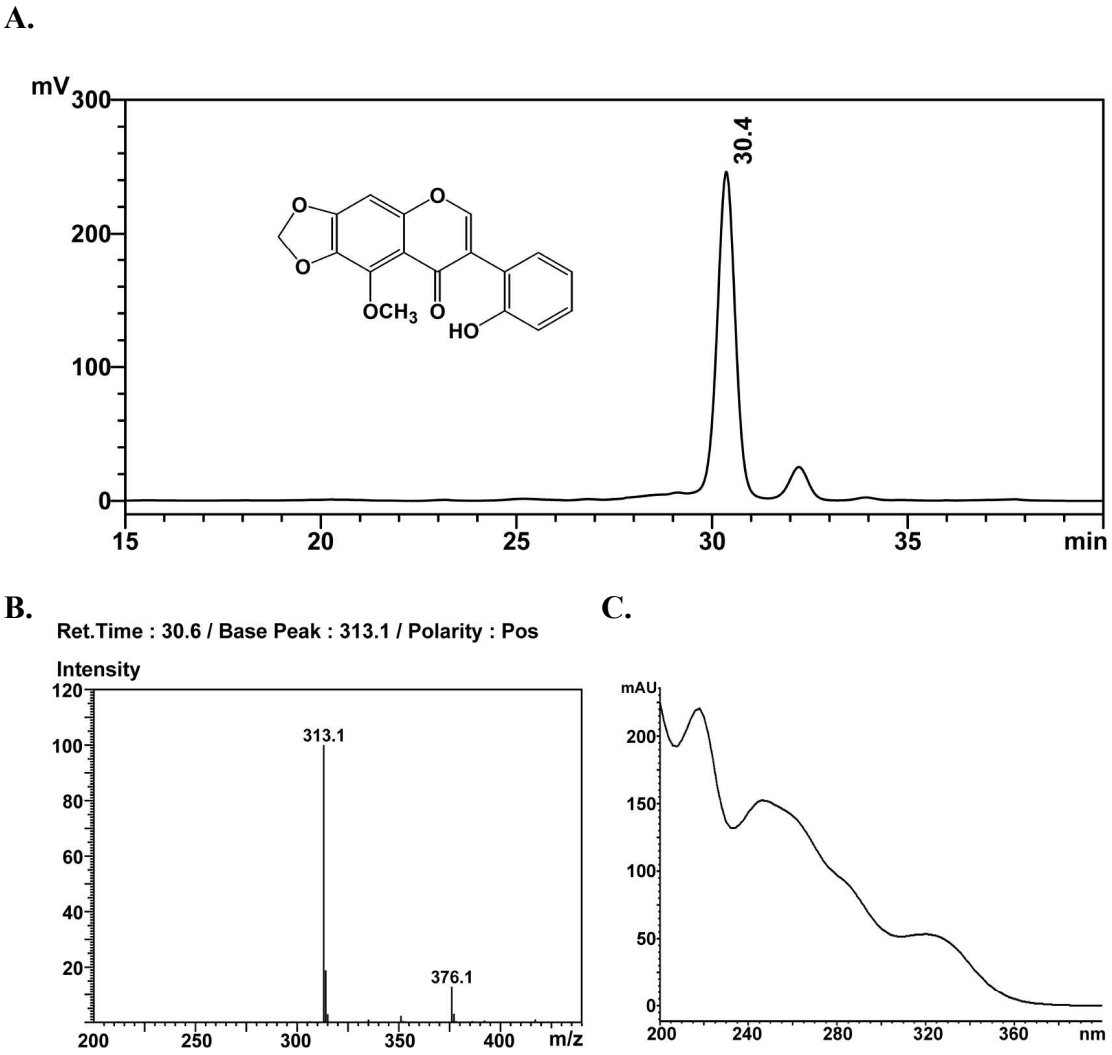

Figure S9. RP-HPLC spectrum (A) with DAD detection and LC-MS analysis (B) for **2**. (C) The UV spectrum from the DAD data.

A.

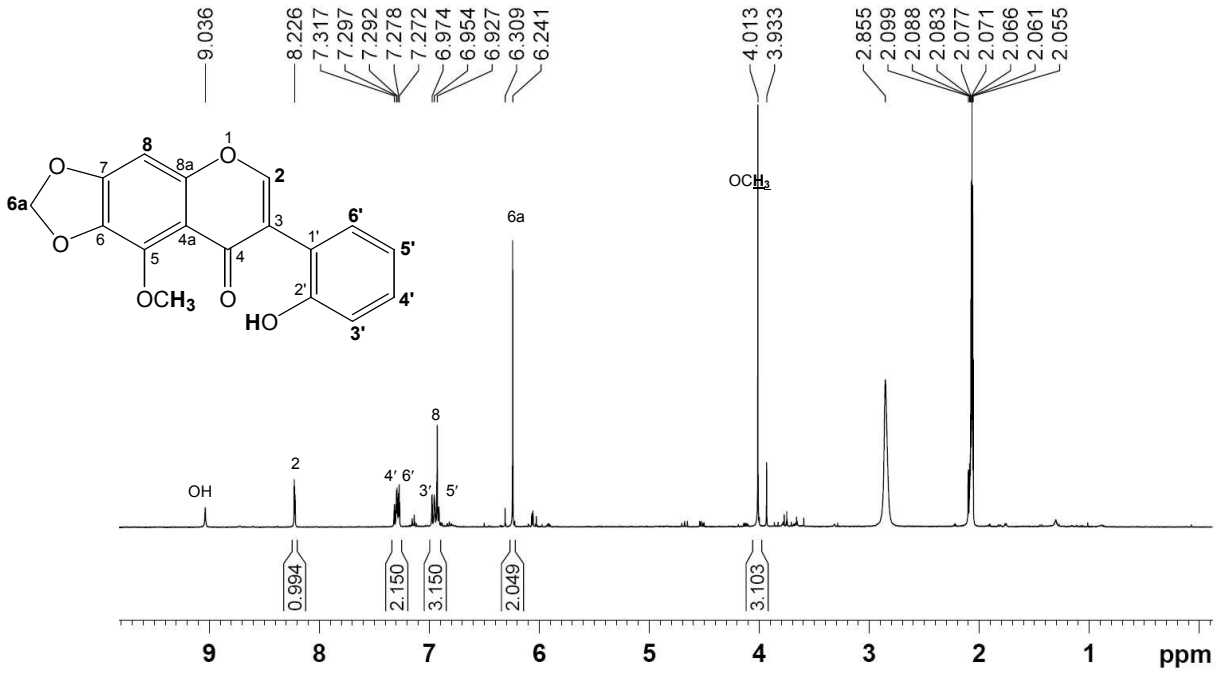

B.

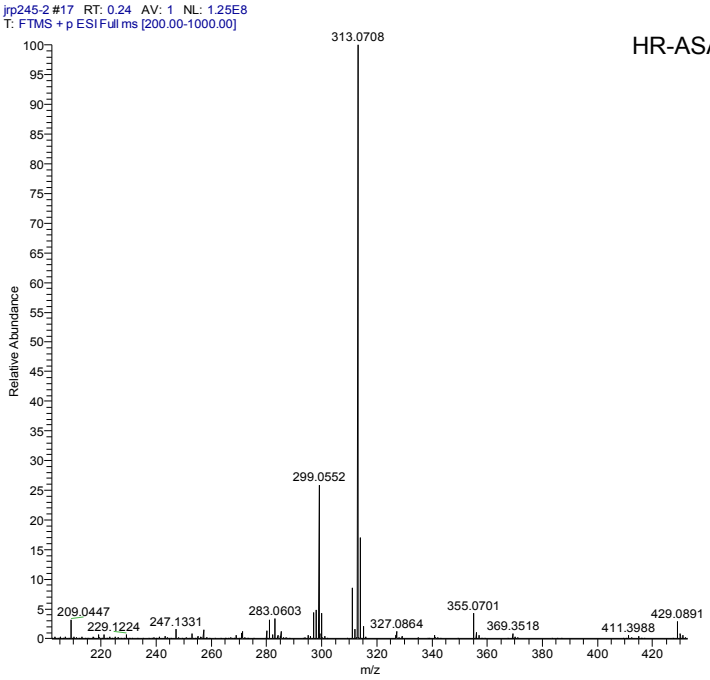

HR-ASAP-MS (ESI, positive ion, *m/z)* 313.0708 $[M+H]^+$

(calculated for $C_{17}H_{13}O_6$, 313.0712)

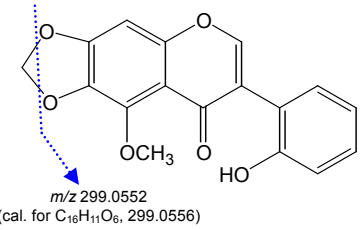

m/z 299.0552

(cal. for $C_{16}H_{11}O_6$, 299.0556)

	$[M+H]^+$	$[M-CH_2]^+$
Found	313.0708	299.0552
Calculated	313.0712	299.0556
Difference	1.59 ppm	1.59 ppm

Figure S10. ^{1}H NMR spectrum (400 MHz, acetone-d_6) (A) and HRMS spectrum (B) for **2**.

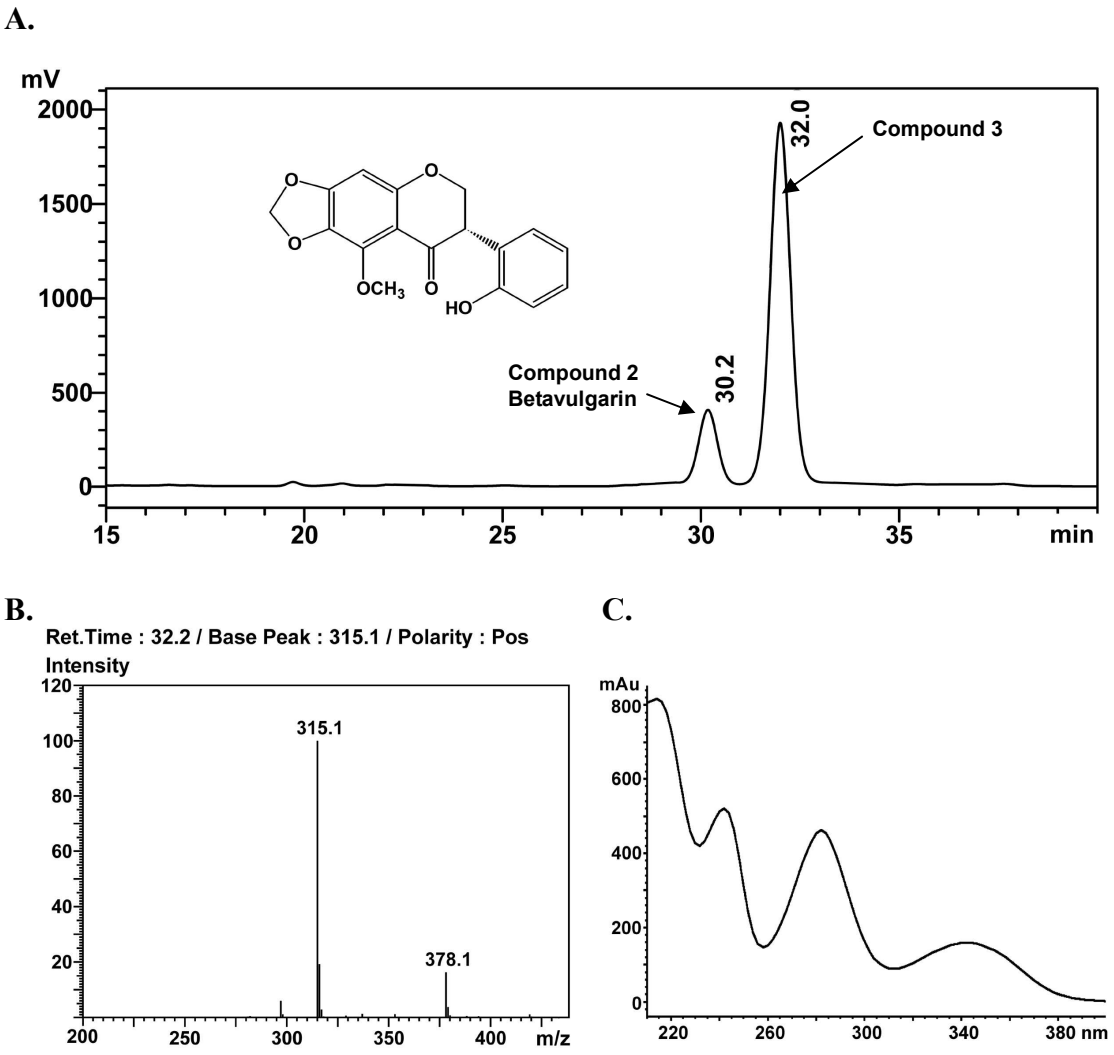

Figure S11. RP-HPLC spectrum (A) with DAD detection and LC-MS analysis (B) for **3**. (C) The UV spectrum from the DAD data.

A.

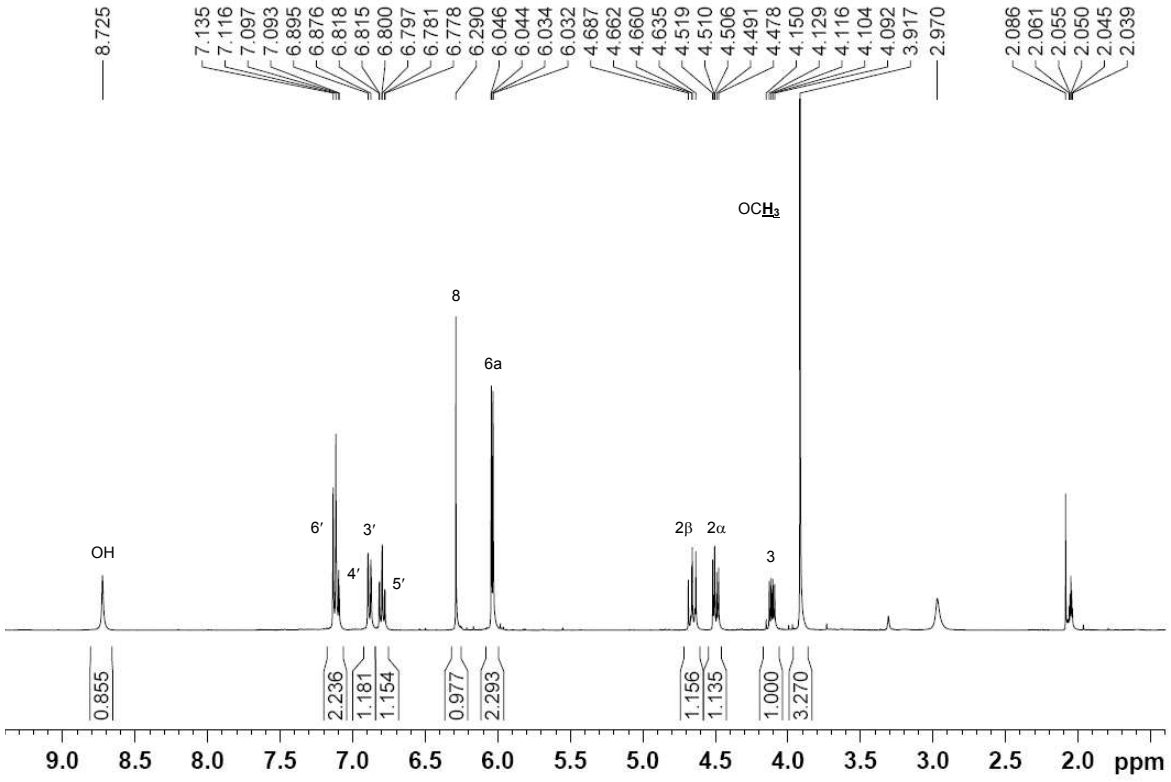

B.

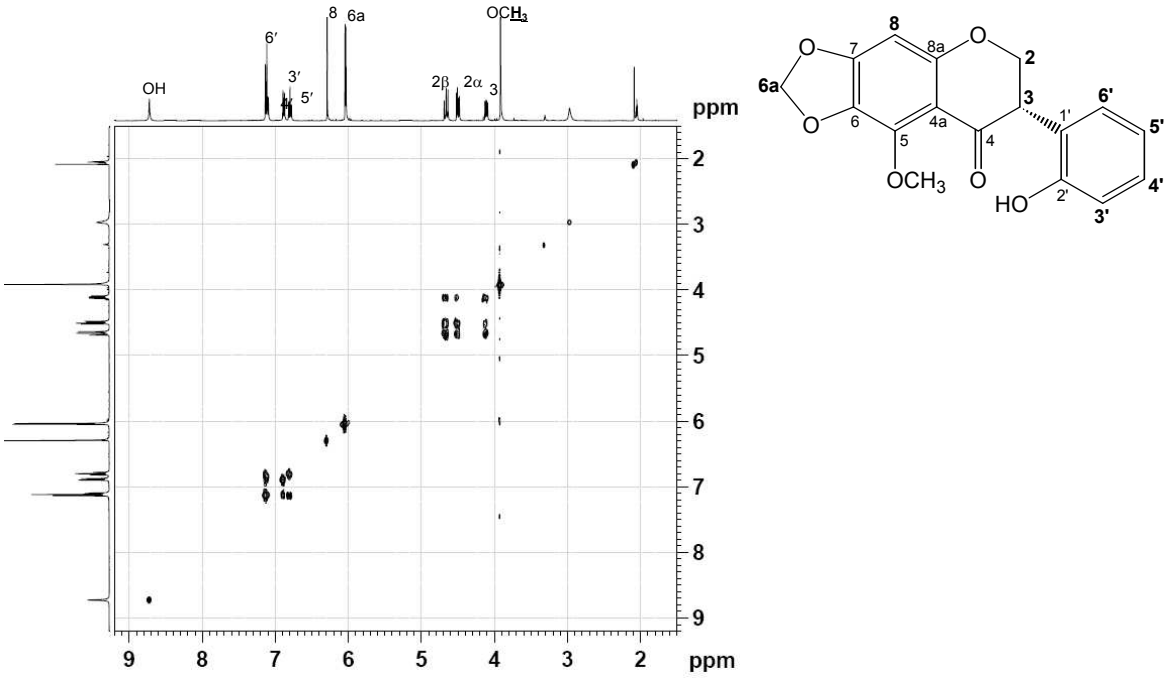

Figure S12. ^{1}H NMR spectrum (A) and ^{1}H-^{1}H COSY spectrum (B) for **3** (400 MHz, acetone-d_6).

A.

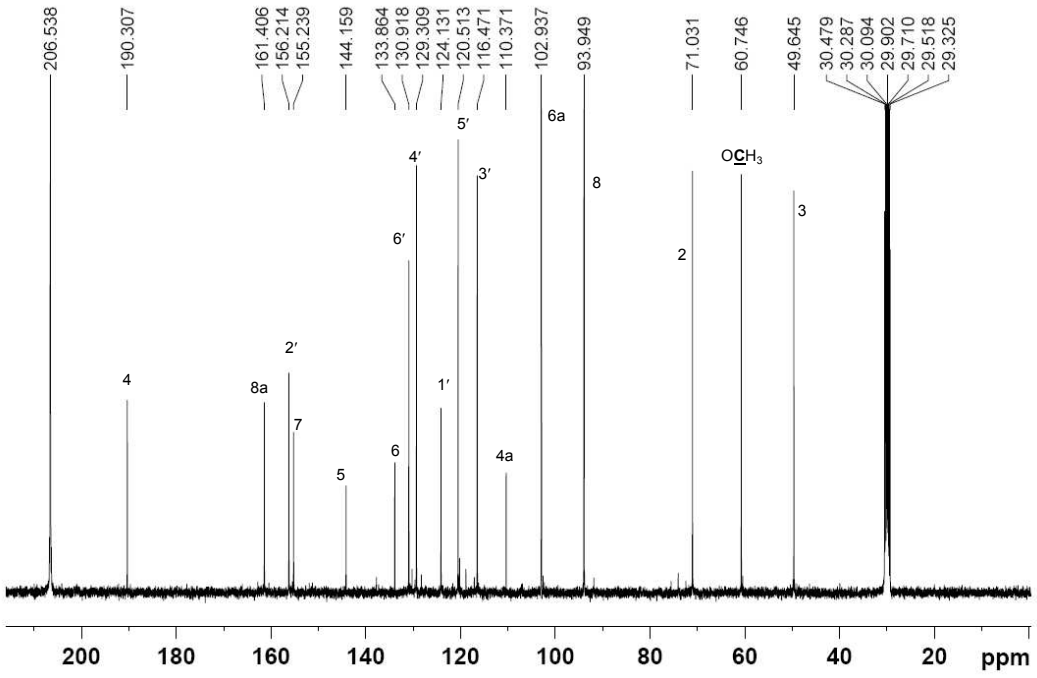

B.

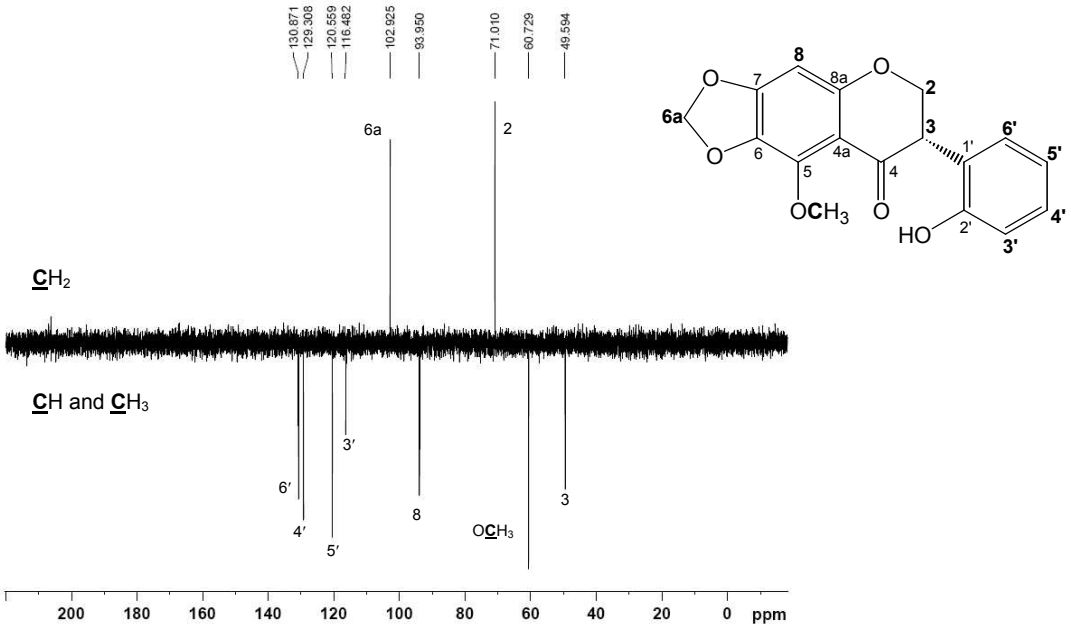

Figure S13. ^{13}C NMR spectrum (A) and DEPT 135 spectrum (B) for **3** (100 MHz, acetone-d_6).

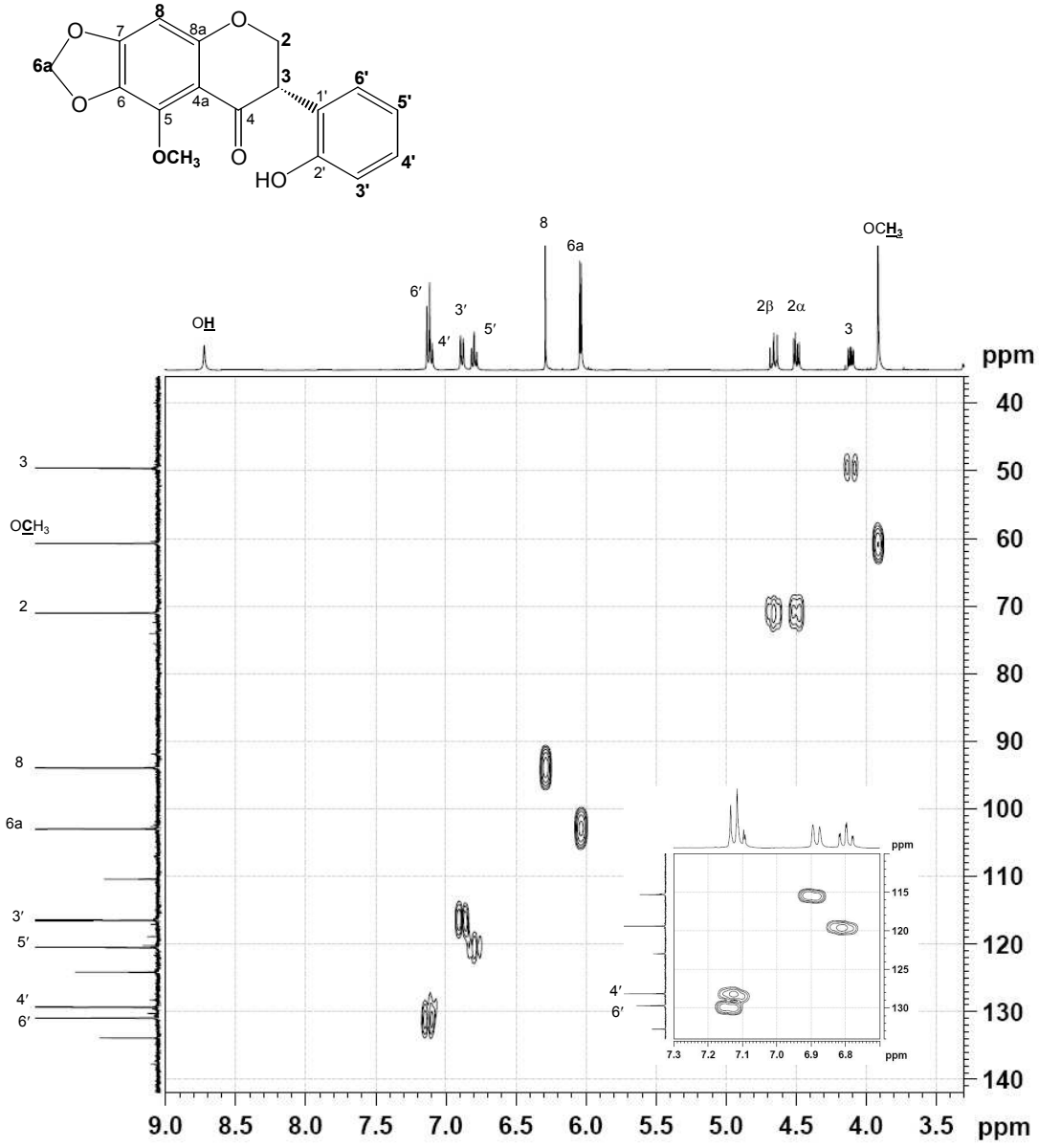

Figure S14. HMQC spectrum for **3** (100 MHz, acetone-d_6).

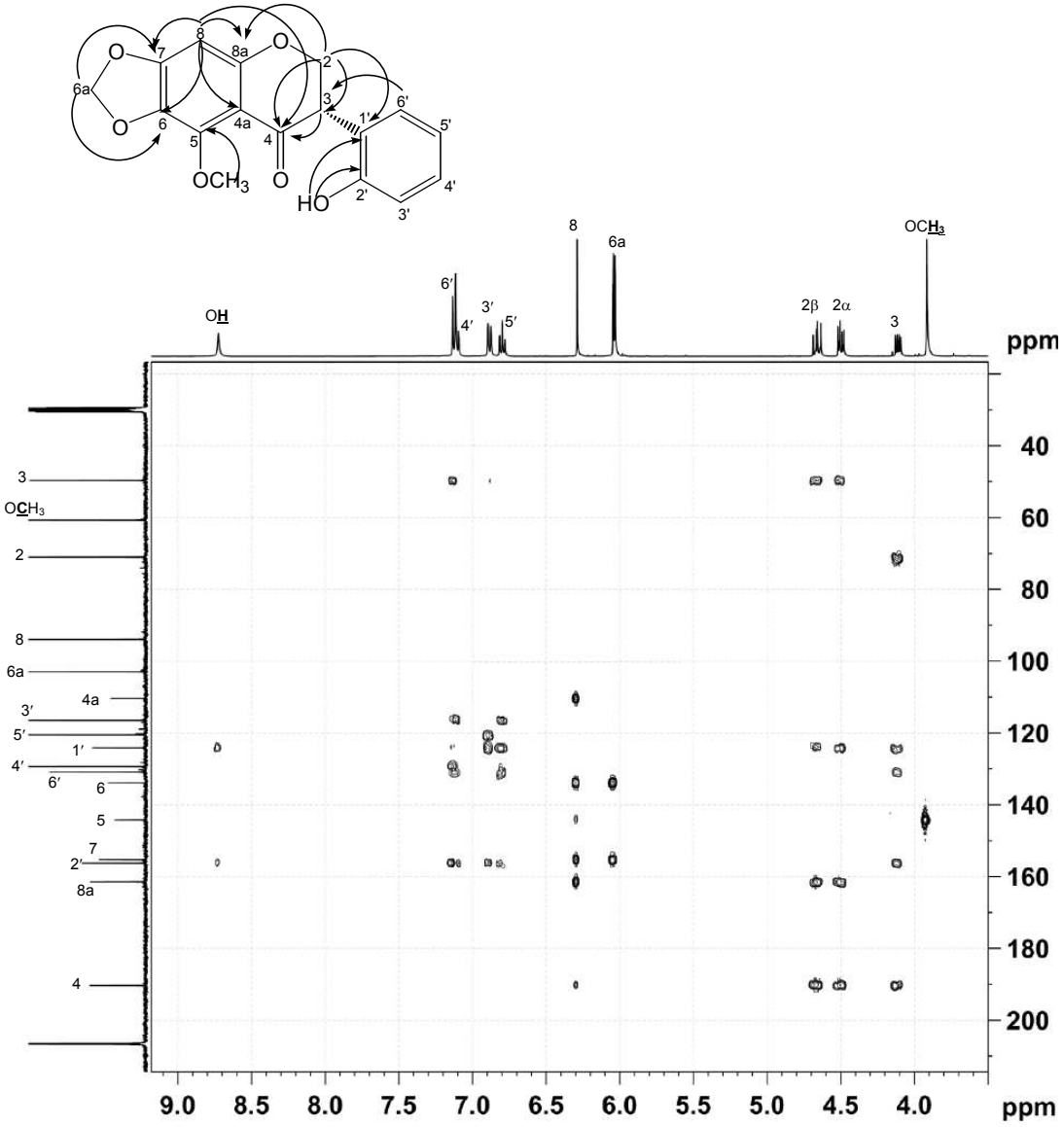

Figure S15. HMBC spectrum for **3** (100 MHz, acetone-d_6). Major interactions are indicated in the compound structure.

A.

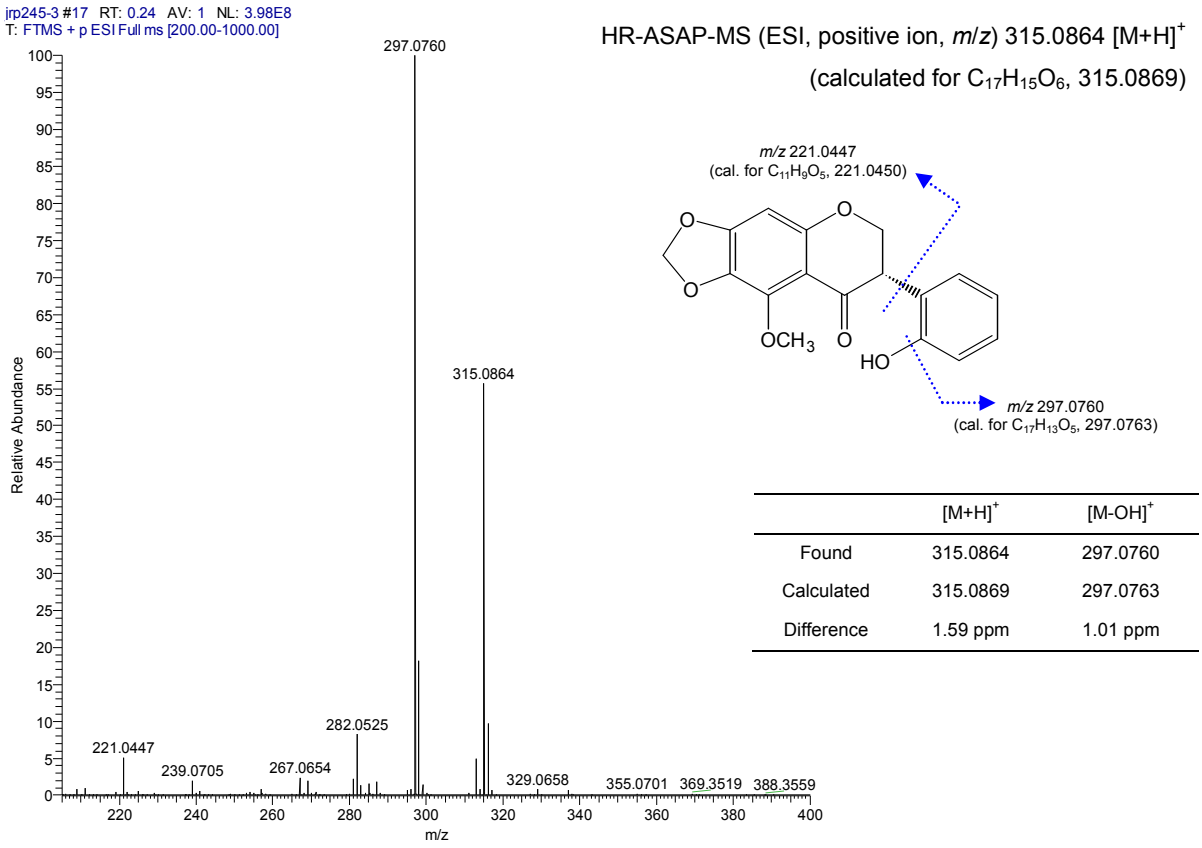

	$[M+H]^+$	$[M-OH]^+$
Found	315.0864	297.0760
Calculated	315.0869	297.0763
Difference	1.59 ppm	1.01 ppm

B.

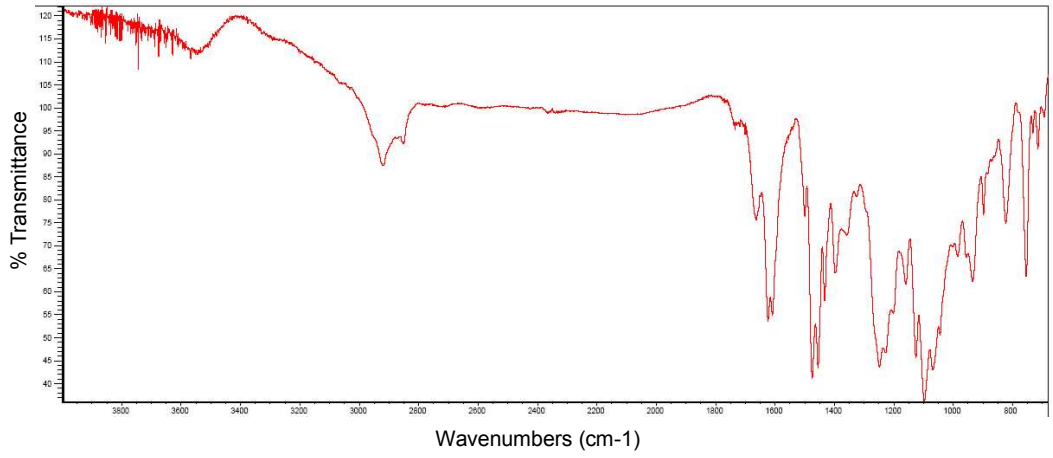

Figure S16. HRMS spectrum (A) and FT-IR spectrum (B) for **3**.

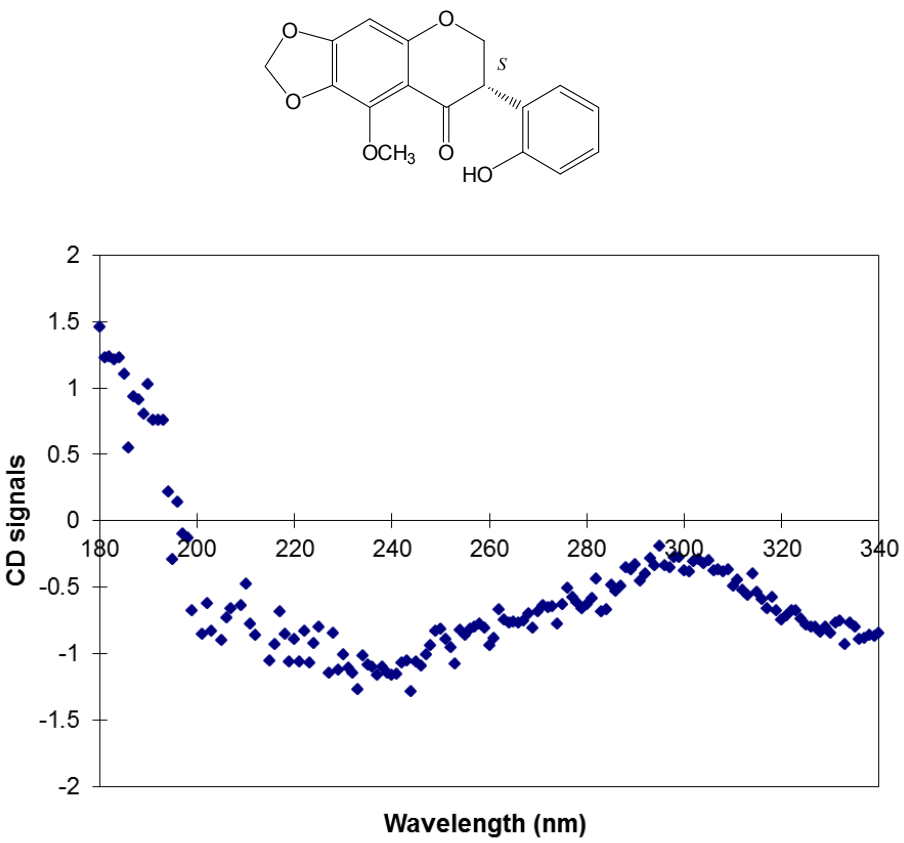

Figure S17. CD spectrum for **3**.

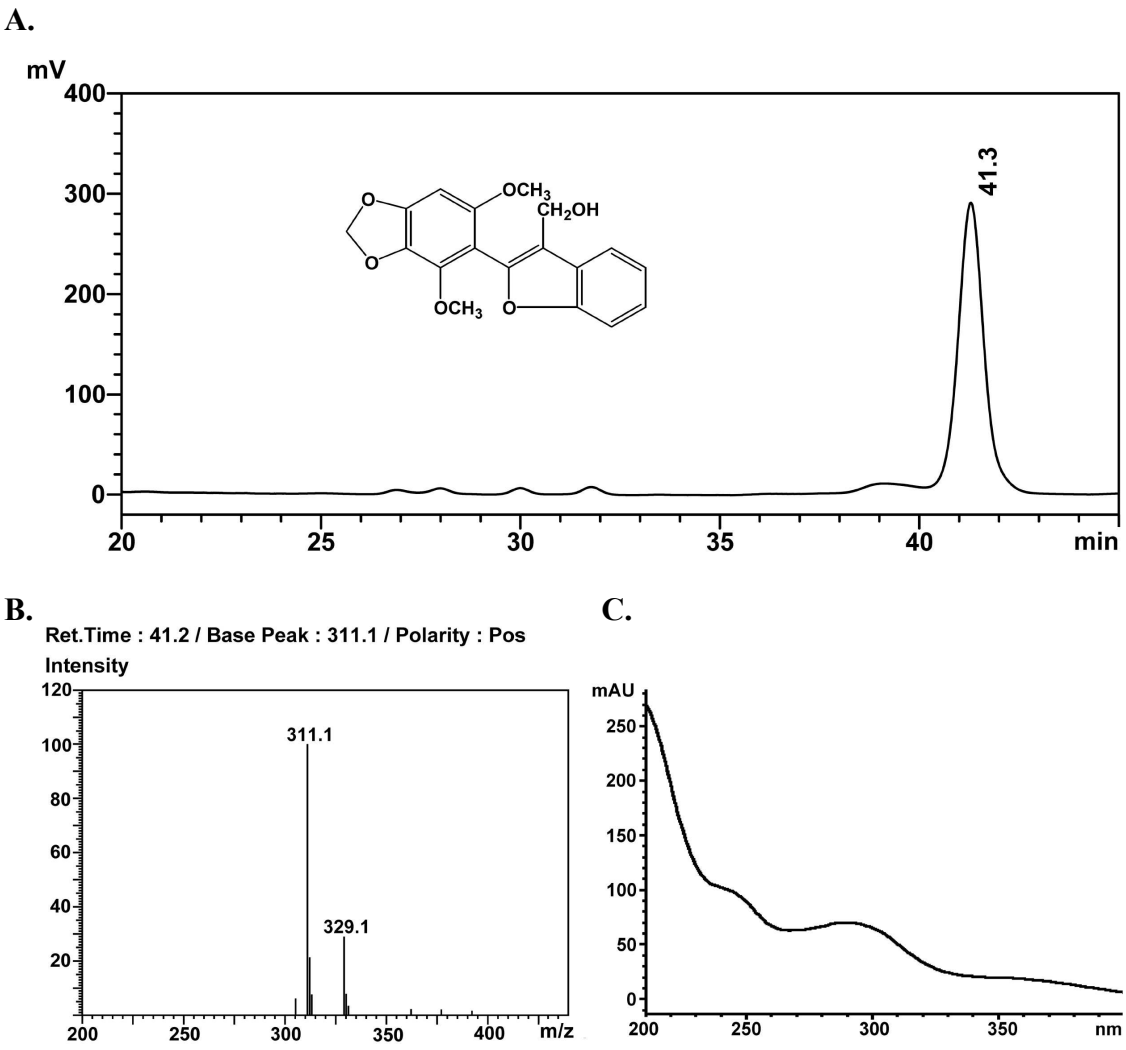

Figure S18. RP-HPLC spectrum (A) with DAD detection and LC-MS analysis (B) for **4**. (C) The UV spectrum from the DAD data.

A.

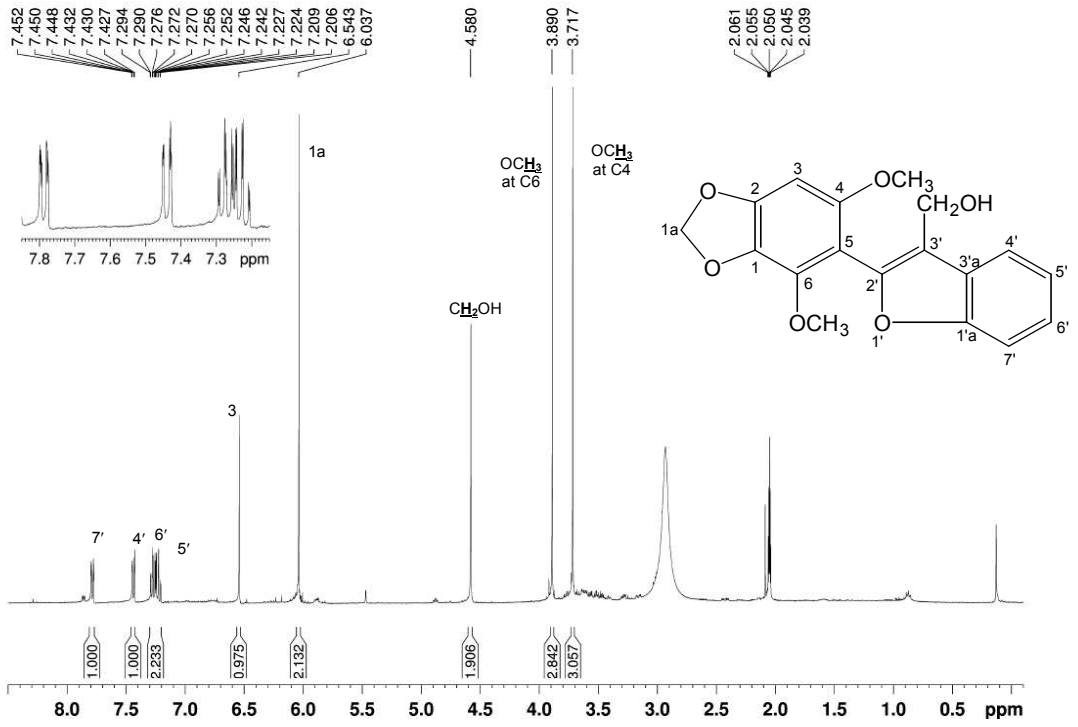

B.

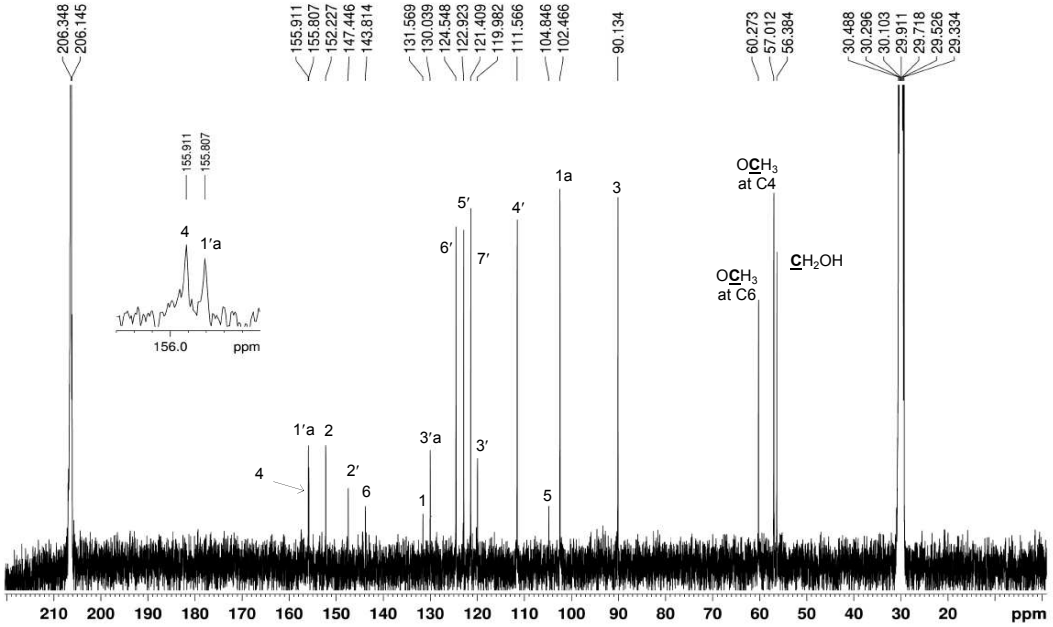

Figure S19. ^{1}H NMR spectrum (400 MHz, acetone-d_6) (A) and ^{13}C NMR spectrum (100 MHz, acetone-d_6) (B) for **4**.

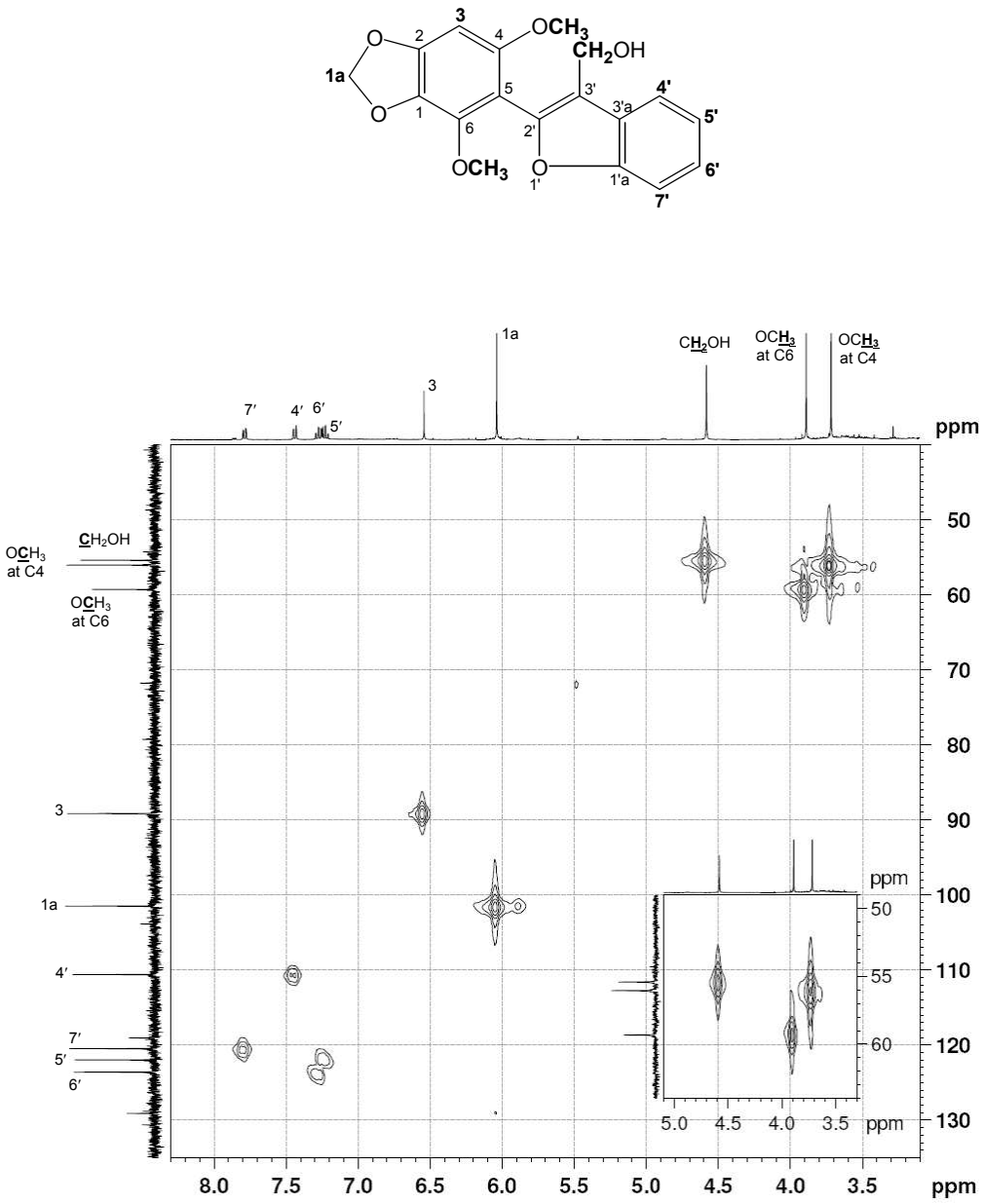

Figure S20. HMQC spectrum for **4** (100 MHz, acetone-d_6).

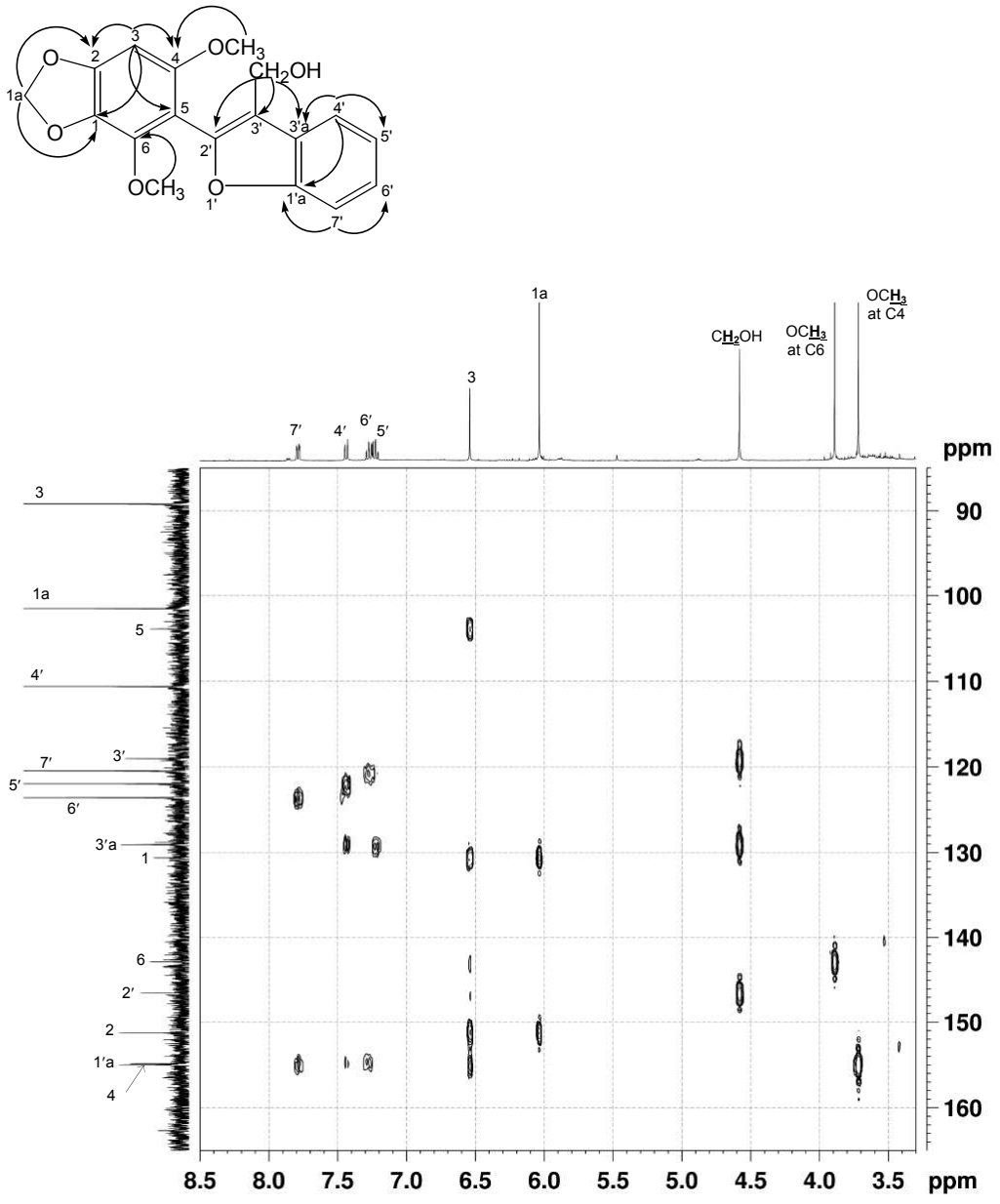

Figure S21. HMBC spectrum for **4** (100 MHz, acetone-d_6). Major interactions are indicated in the compound structure.

A.

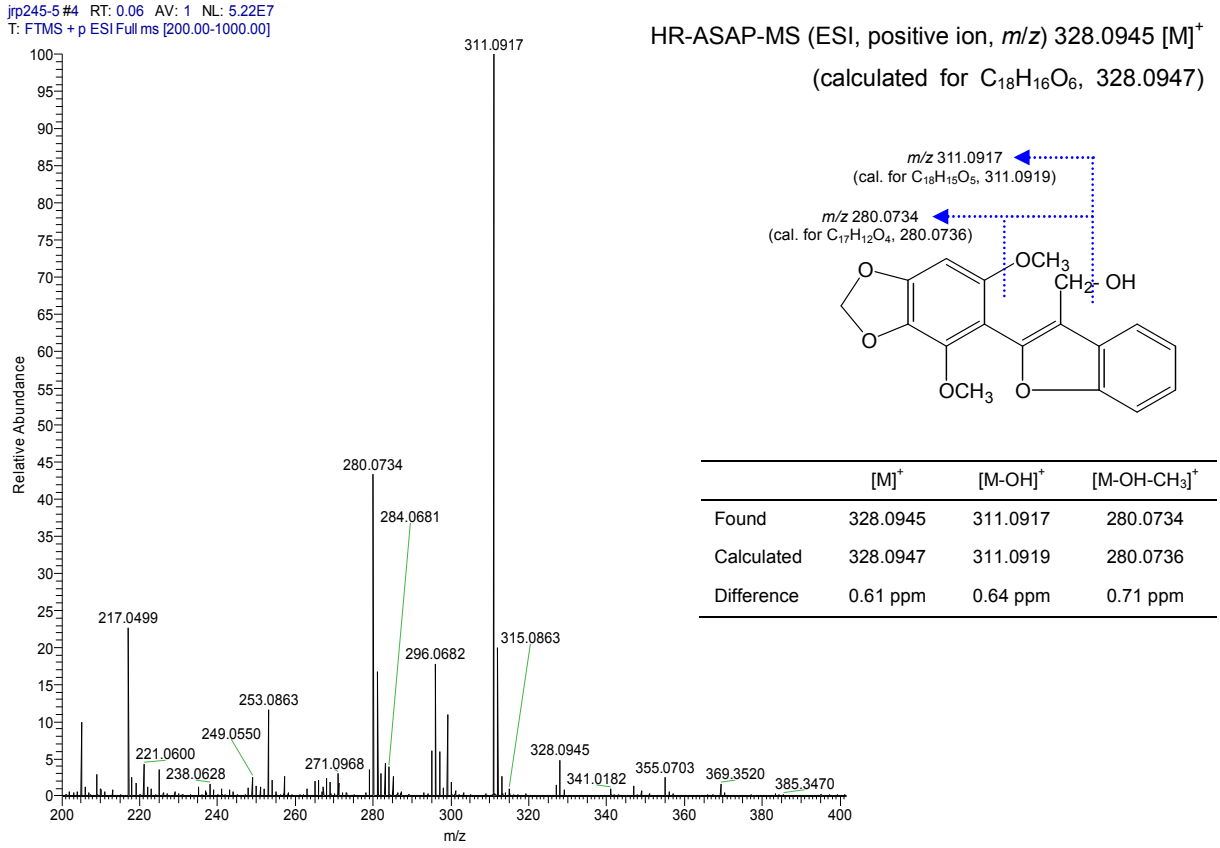

	$[M]^+$	$[M\text{-}OH]^+$	$[M\text{-}OH\text{-}CH_3]^+$
Found	328.0945	311.0917	280.0734
Calculated	328.0947	311.0919	280.0736
Difference	0.61 ppm	0.64 ppm	0.71 ppm

B.

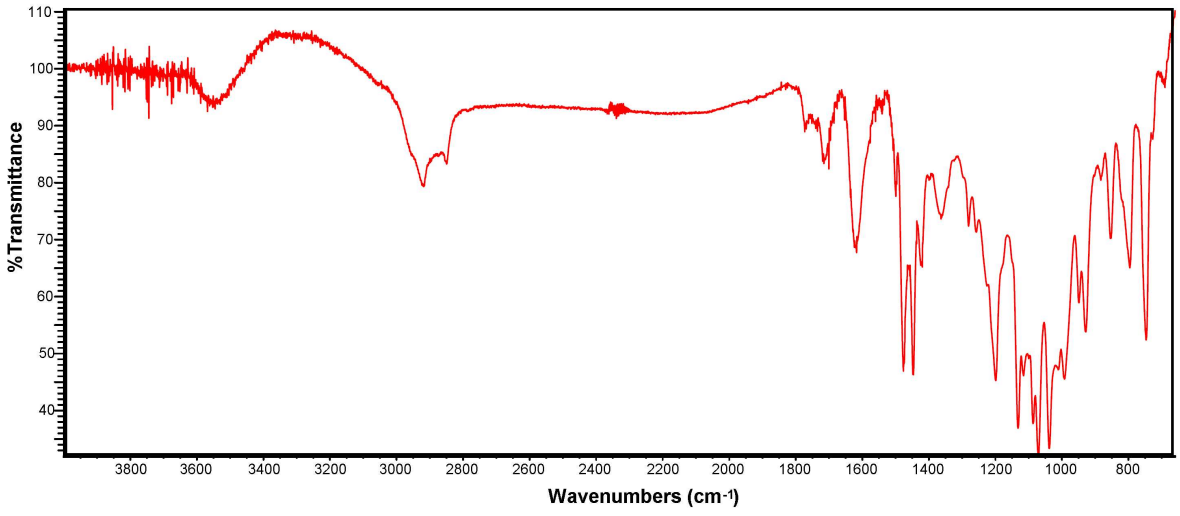

Figure S22. HRMS spectrum (A) and FT-IR spectrum (B) for **4**.

A.

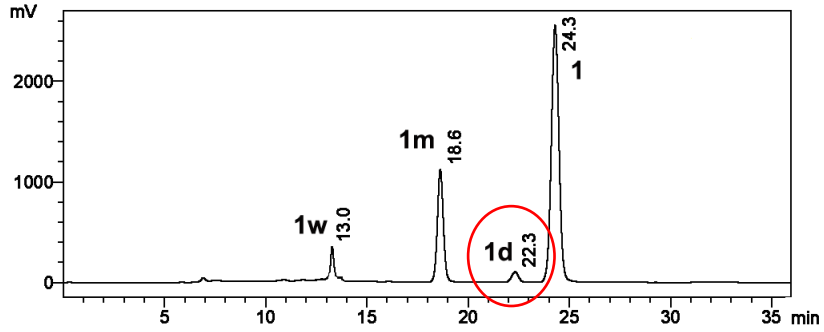

B.

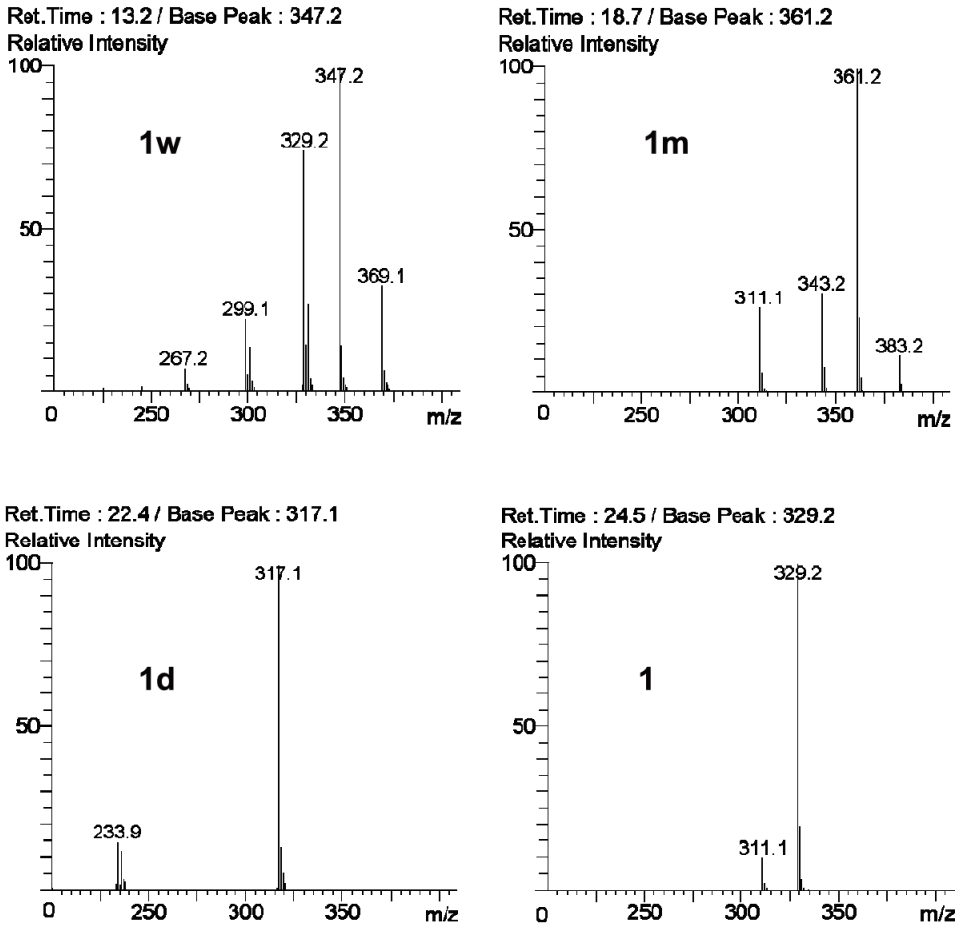

Figure S23. LC-MS (ESI, positive mode, *m/z*) analysis of the water adduct **1w**, MeOH adduct **1m**, **1**, and **1d** in the water/MeOH/ACN (4:3:3, v/v/v) mobile phase. (A) LC chromatogram with retention times of the compound peaks. (B) MS analysis for each peak shown in the LC chromatogram.

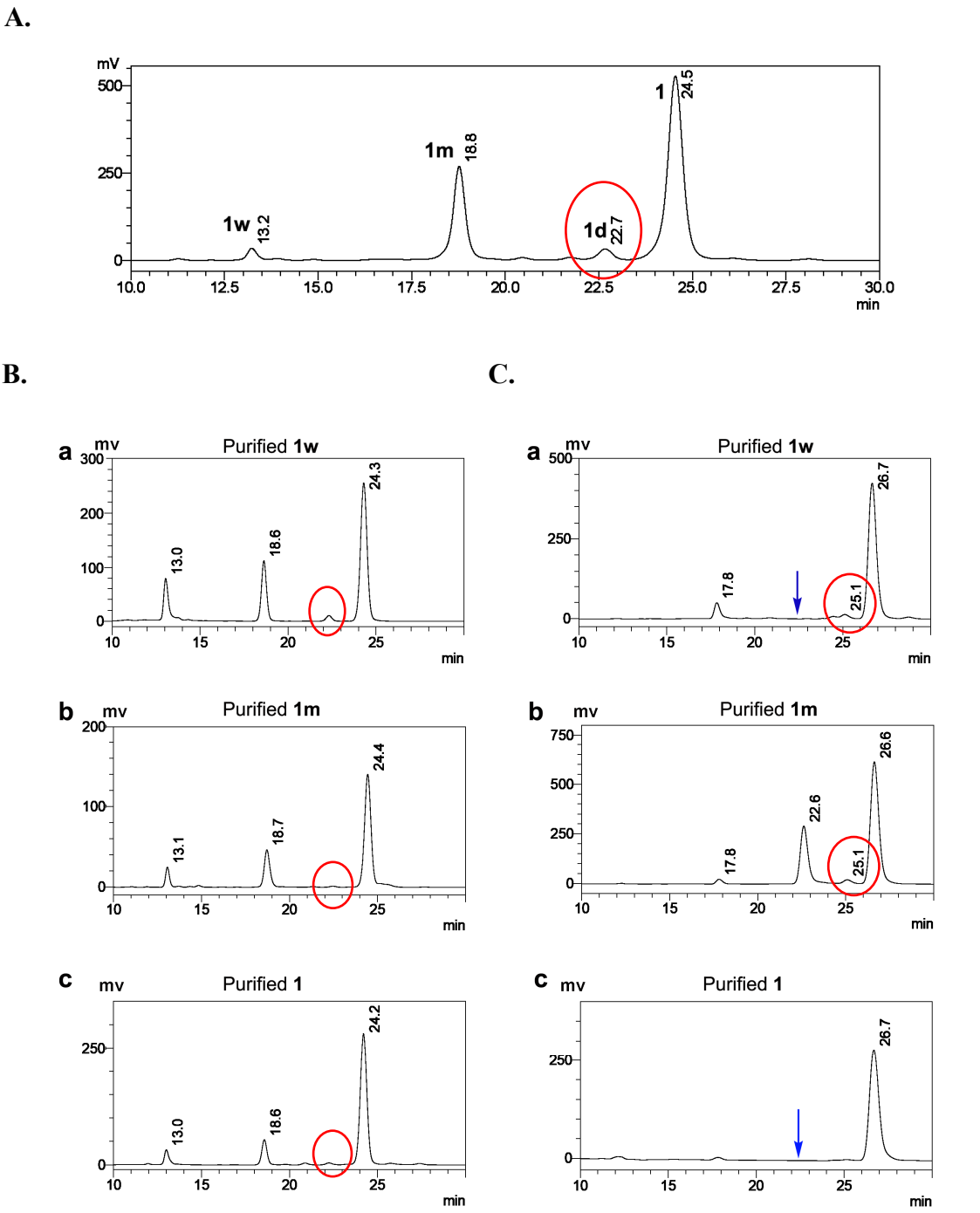

Figure S24. RP-HPLC analysis of the water adduct **1w** (a), MeOH adduct **1m** (b), and **1** (c) purified in the EtOH-based solvent. (A) LC chromatogram prior to purification of all compounds. (B) LC chromatogram analyzed in the water/MeOH/ACN (4:3:3, v/v/v) mobile phase with each of the purified compounds. (C) LC chromatograms analyzed in the water/EtOH/ACN (4:3:3, v/v/v) mobile phase with each of the purified compounds. The blue arrows are the positions for **1m**, which was detected only in the use of MeOH-based solvent. The red circles are for **1d**.

A.

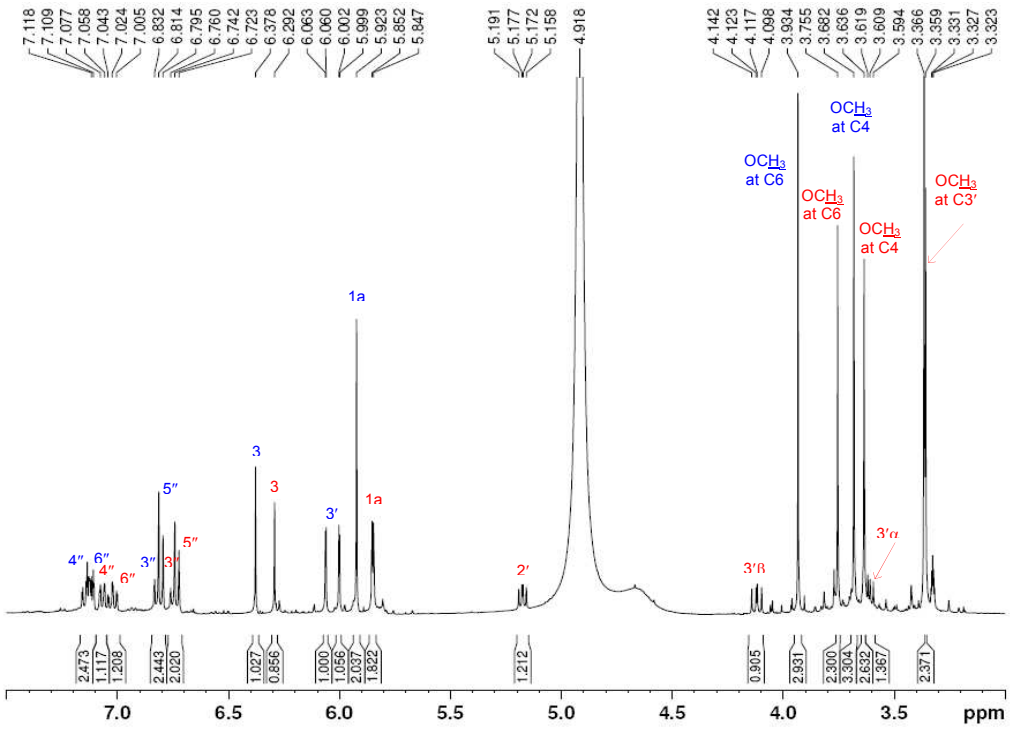

B.

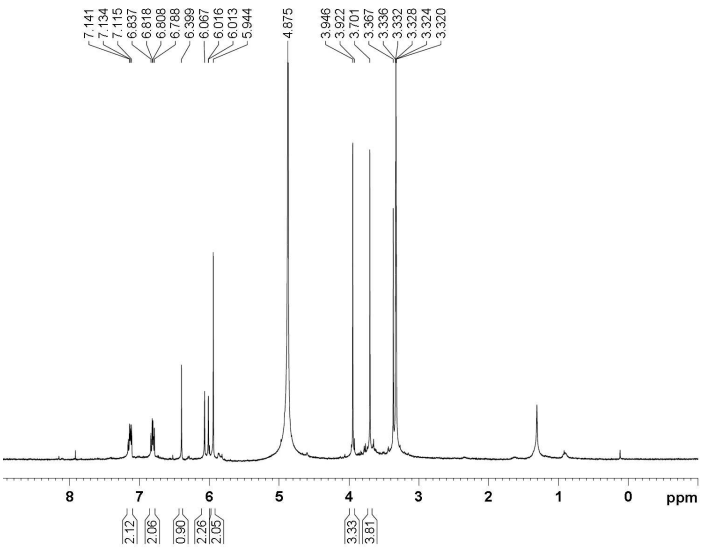

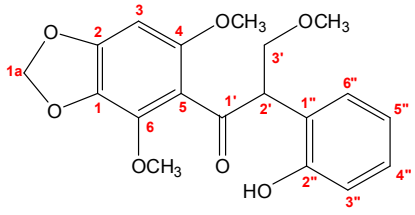

1m

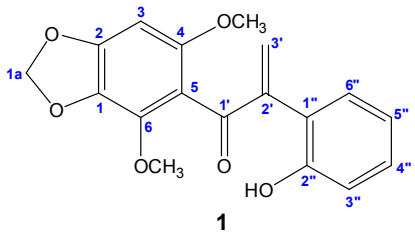

1

Figure S25. ^{1}H NMR spectrum for MeOH adduct **1m** and **1** (400 MHz, CD_3OD). The CD_3OD lock solvent was used to maximize the yield for the NMR experiment. (A) ^{1}H NMR spectrum of a mixture o f the MeOH **adduct 1m (red) and 1 (blue). (B)** ^{1}H NMR spectrum for **1** purified in the EtOH-based RP-HPLC (400 MHz, CD_3OD).

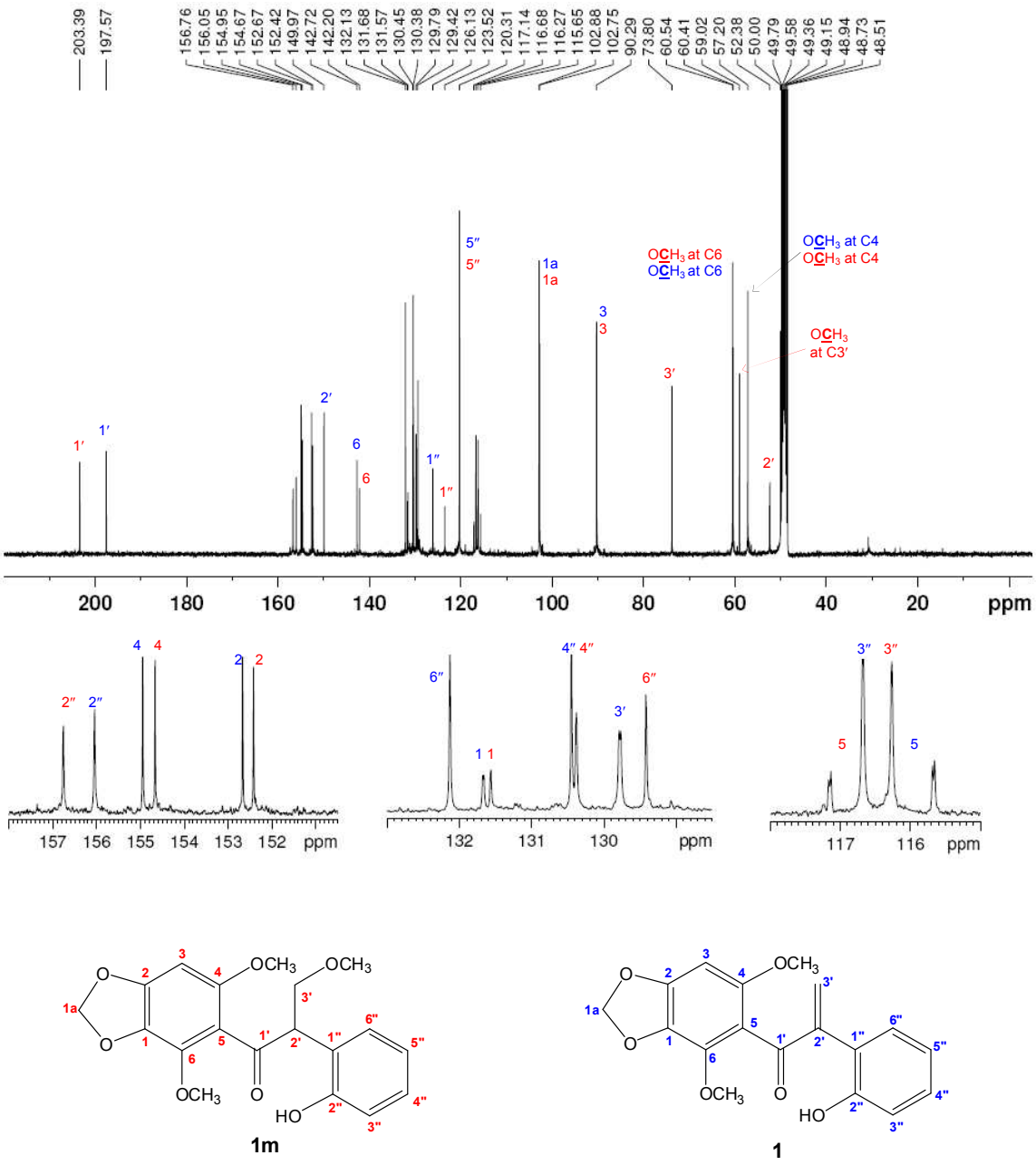

Figure S26. ^{13}C NMR spectrum for a mixture of the MeOH adduct **1m (red)** and **1 (blue)** (100 MHz, CD_3OD).

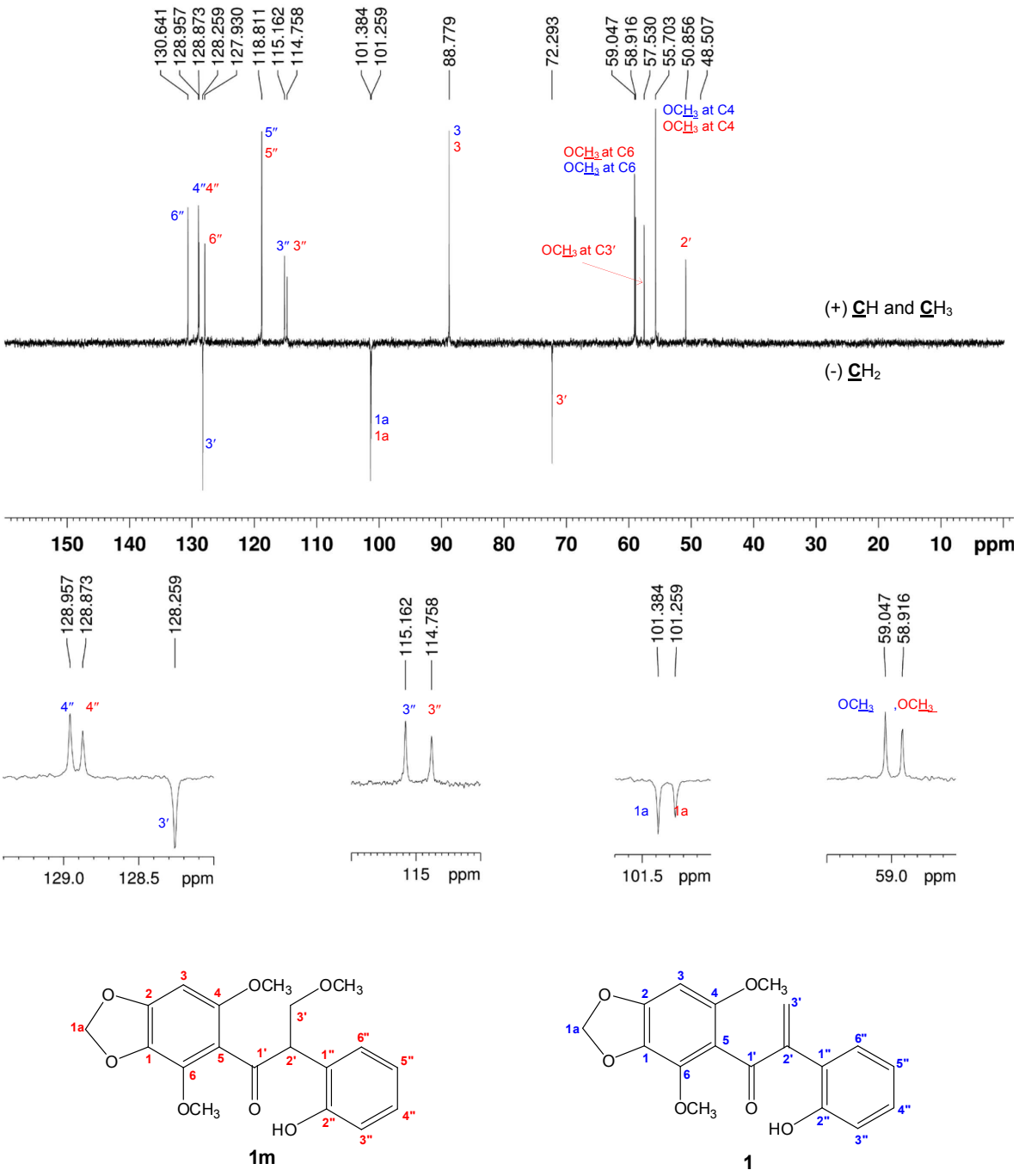

Figure S27. DEPT135 spectrum for a mixture of the MeOH adduct **1m (red)** and **1** (blue) (100 MHz, CD_3OD).

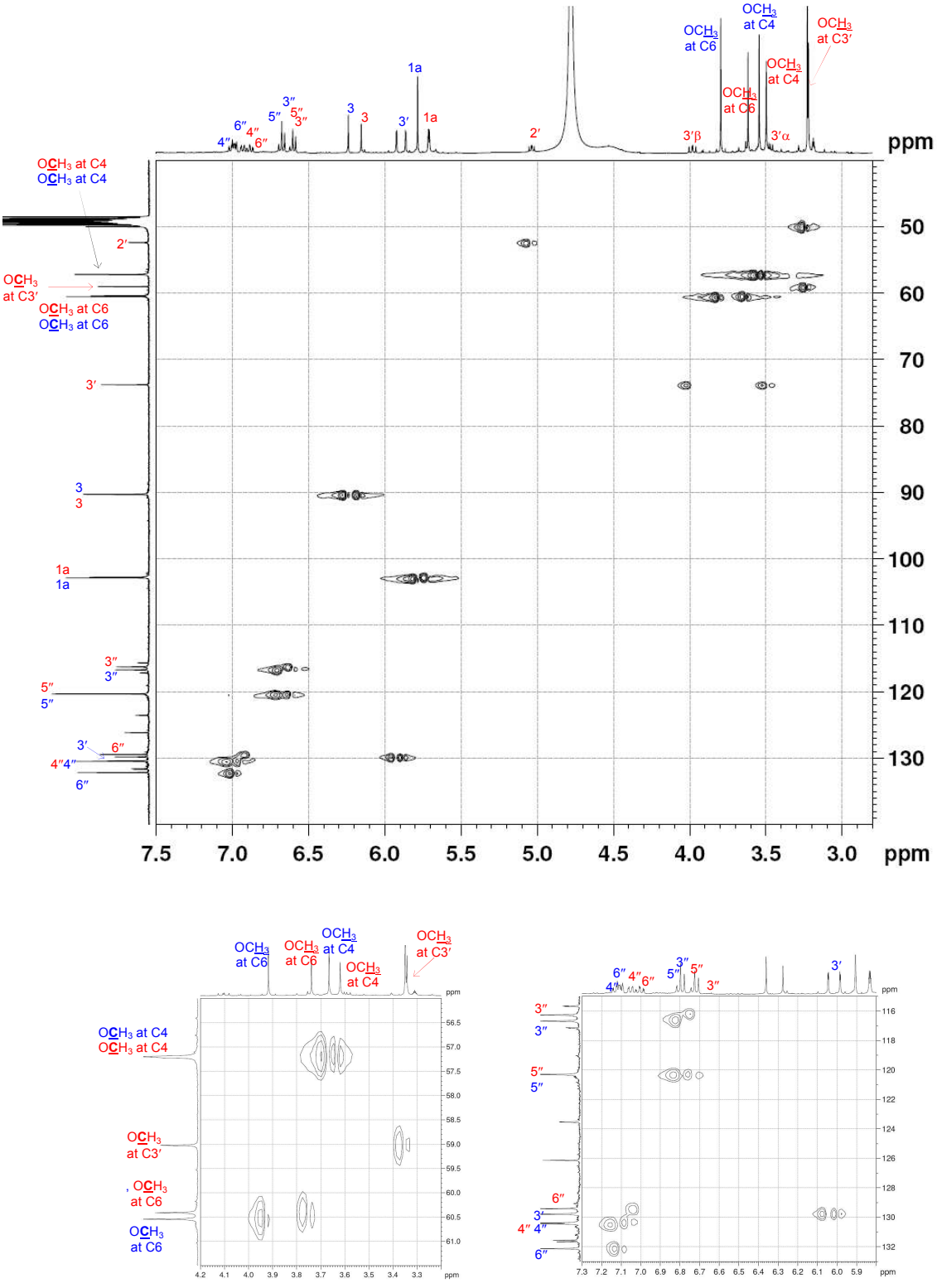

Figure S28. HSQC spectrum for a mixture of the MeOH adduct **1m (red)** and **1 (blue)**(100 MHz, CD_3OD).

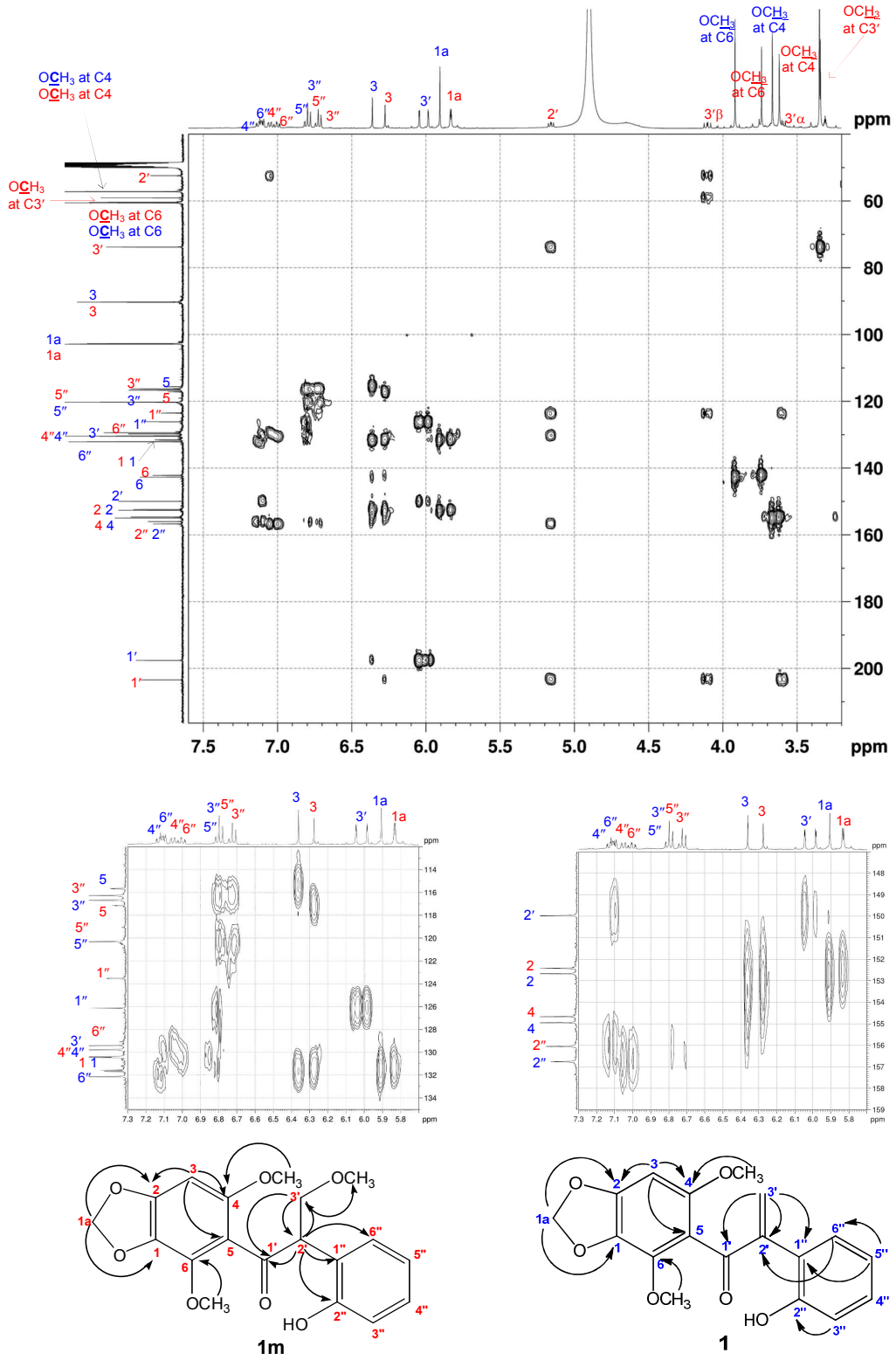

Figure S29. HMBC spectra for a mixture of the MeOH adduct **1m** (red) and **1** (blue) (100 MHz, CD_3OD). Major interactions are indicated in the compound structures.

A. B.

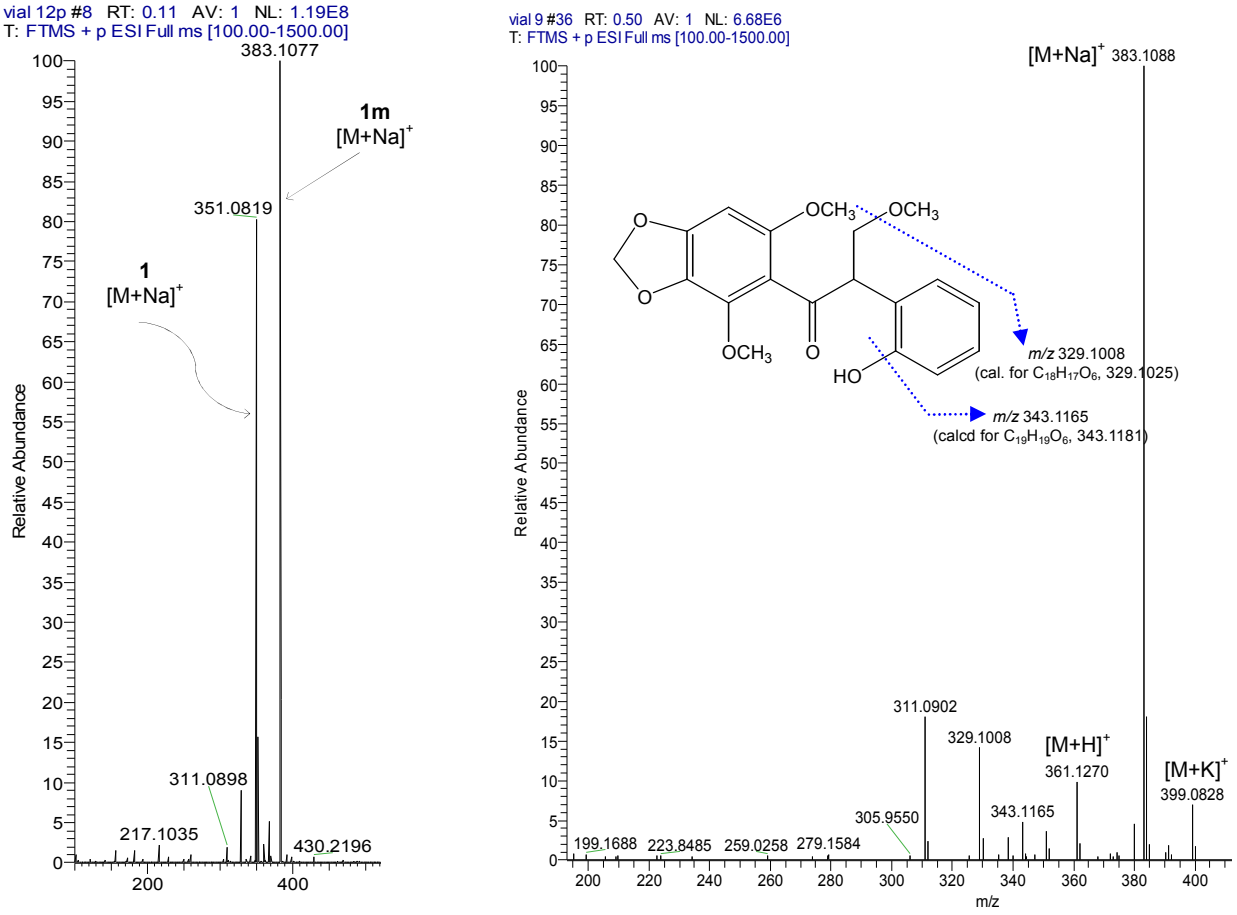

Compound **1m**

HRMS (ESI, positive mode, *m/z*)

383.1077 $[M+Na]^+$

(calculated for $C_{19}H_{20}NaO_7$, 383.1107)

Compound **1**

HRMS (ESI, positive mode, *m/z*)

351.0819 $[M+Na]^+$

(calculated for $C_{18}H_{16}NaO_6$, 351.0844)

Compound **1m**

HRMS (ESI, positive mode, *m/z*)

361.1270 $[M+H]^+$

(calculated for $C_{19}H_{21}O_7$, 361.1287)

383.1088 $[M+Na]^+$

(calculated for $C_{19}H_{20}NaO_7$, 383.1107)

399.0828 $[M+K]^+$

(calculated for $C_{19}H_{20}KO_7$, 399.0846)

Figure S30. HRMS spectrum of a mixture of **1m** and **1**. (A) MS spectrum for a mixture of **1m** and **1** in MeOH carrier solvent. (B) MS spectrum for **1m**, the MeOH adduct, extracted from (A) spectrum data.

A.

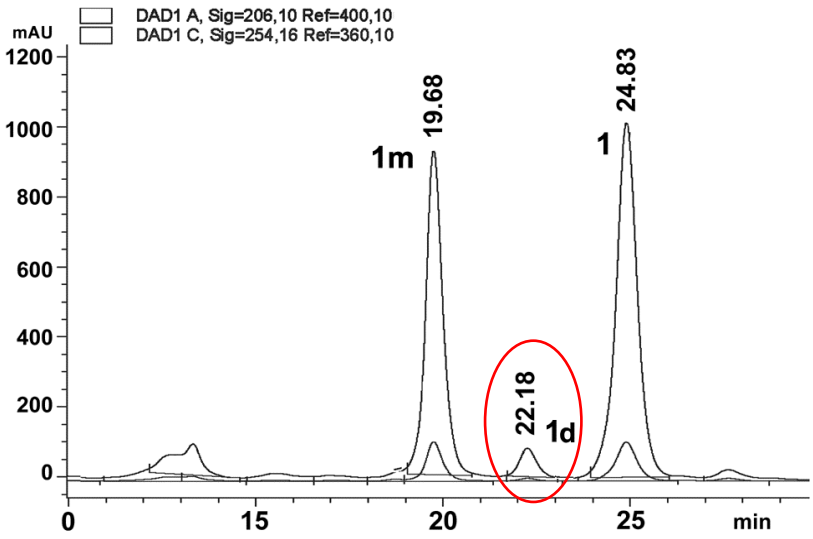

B.

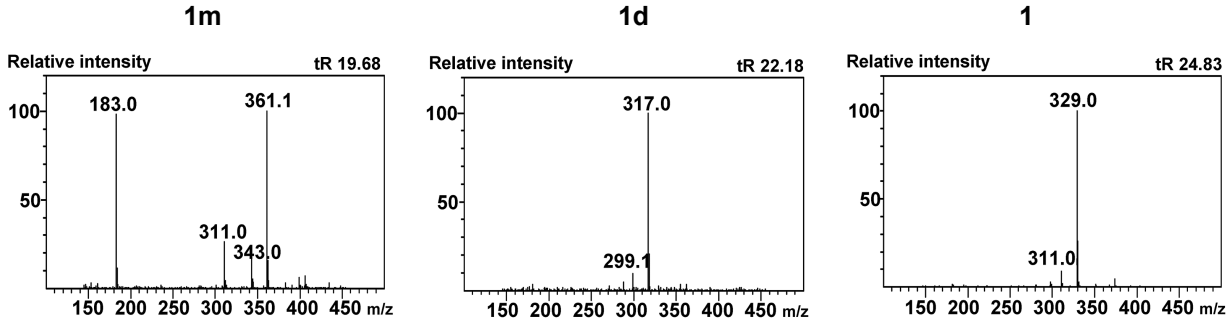

Figure S31. LC-MS (ESI, positive mode, *m/z*) analysis of the minor peak **1d** (red open circle) with **1m** and **1**. (A) LC chromatogram in water/ACN (1:1, v/v) mobile phase and flow rate 0.3 mL·min^{-1}. (B) MS analysis of the LC chromatogram: **1m** (t_R 19.68 min), **1d** (t_R 22.18 min), and **1** (t_R 24.83 min). The minor peak at t_R 22.18 min was collected to identify the chemical structure of **1d**.

A.

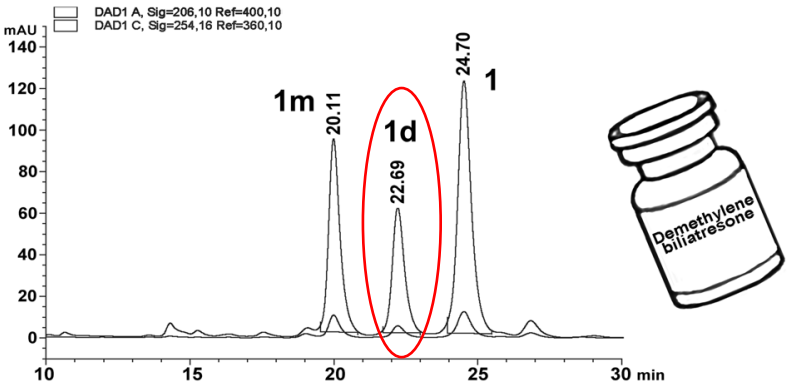

B.

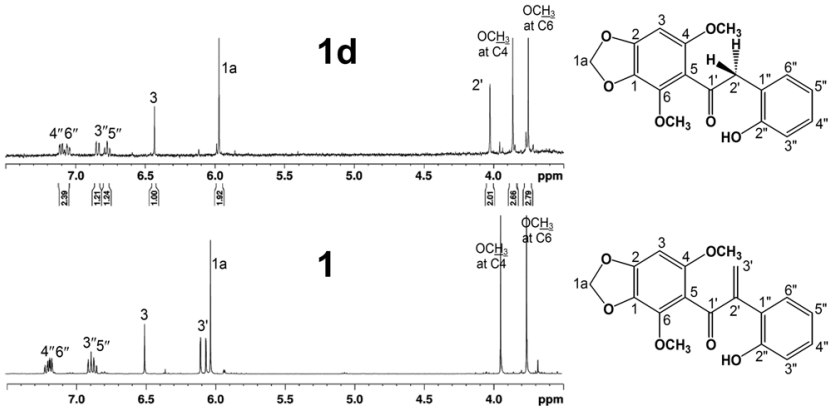

C.

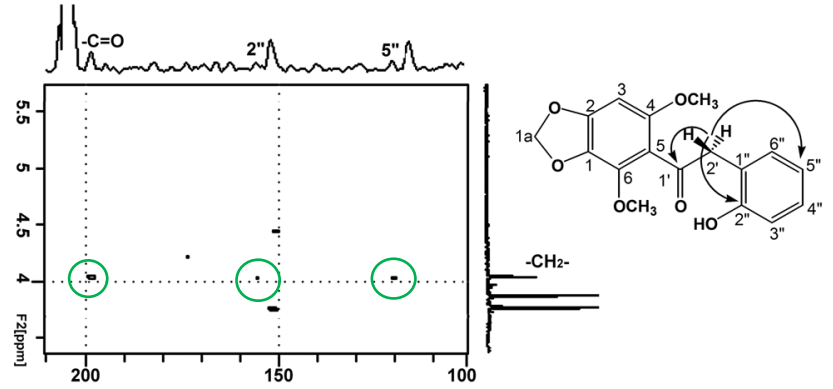

Figure S32. Purification and identification of the chemical structure of **1d**. (A) RP-HPLC chromatogram after conversion of **1d**, caused by addition of MeOH, to **1m** (t_R 20.11 min) and **1** (t_R 24.70 min). The peak **1d** (t_R 22.69 min) was purified with the water/ACN solvent. (B) ^{1}H NMR spectrum (400MHz, acetone-d_6) of the purified **1d** and comparison with that of **1**. (C) HMBC spectrum (100MHz, acetone-d_6) of the purified **1d**. Major HMBC correlations of the ethanone bridge (-CH_2-) signals indicated with the green circles.

A.

B.

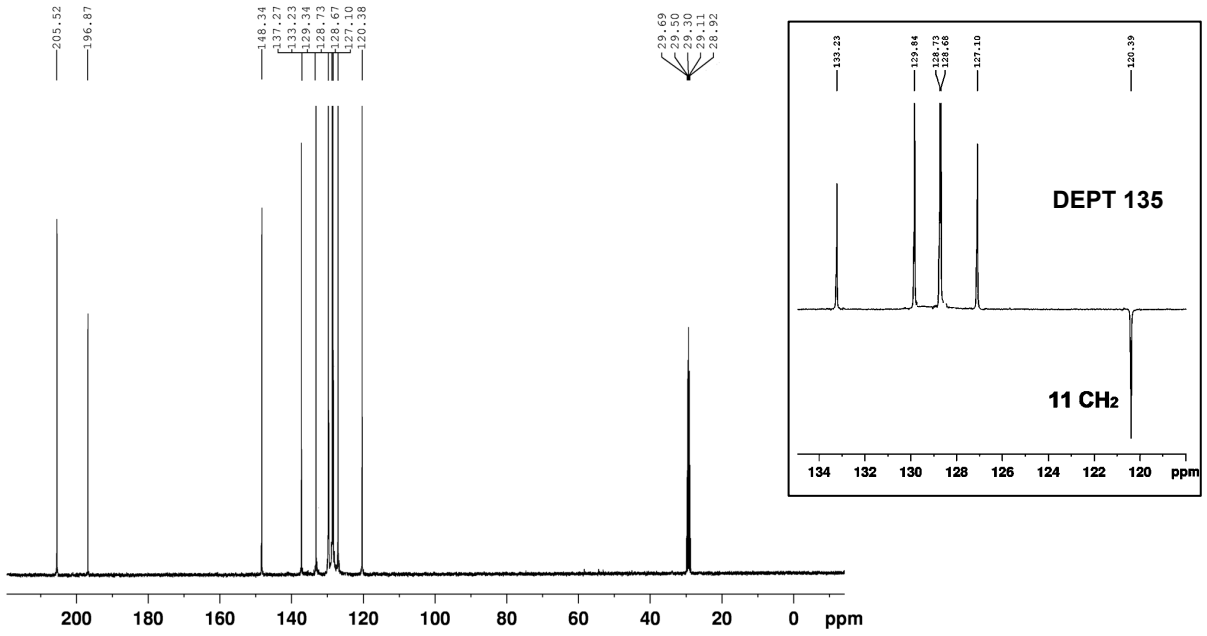

Figure S33. NMR spectra for the synthetic **5**. (A) ^{1}H NMR spectrum (400 MHz, acetone-d_6) and (B) ^{13}C NMR and DEPT135 spectra (100 MHz, acetone-d_6). The DEPT135 spectrum showed CH_2 peak of a methylene carbon (δ_C=120.4 ppm, C11).

A.

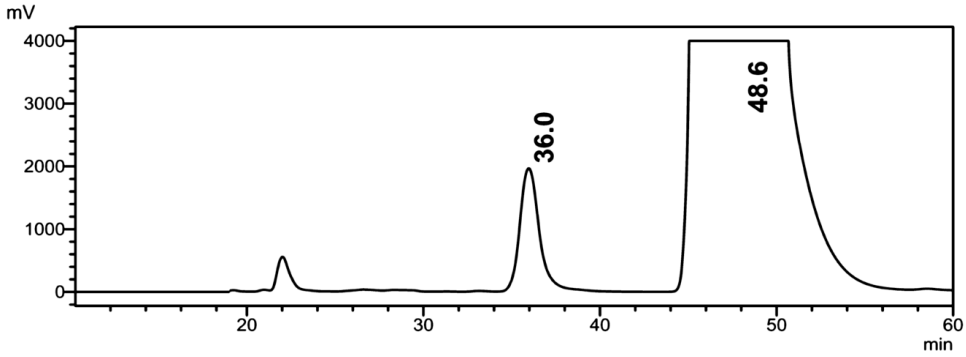

B.

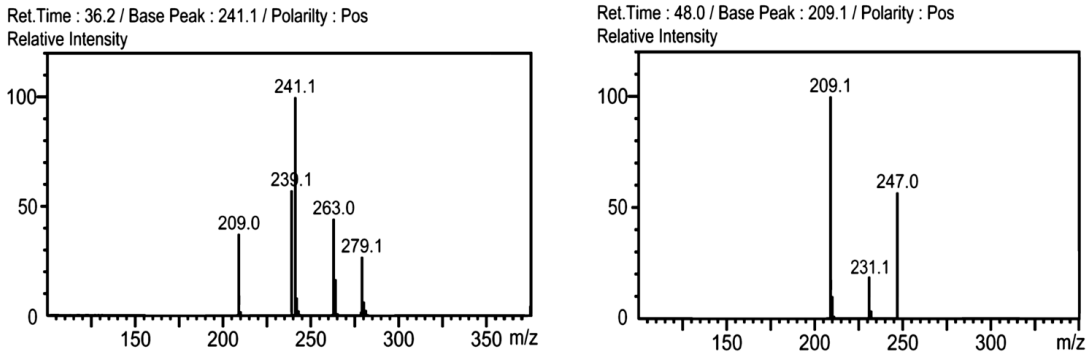

Figure S34. LC-MS (ESI, positive mode, *m/z*) analysis of the synthetic **5**. (A) LC chromatogram of **5** in the water/MeOH/ACN solvent. Two peaks appeared at the retention times of t_R 36.0 and t_R 48.6 min, respectively. (B) MS analysis of the two peaks shown in the LC chromatogram. The peak at t_R 36.0 showed a mass at *m/z* 241 $[M+H]^+$, 263 $[M+Na]^+$, and 279 $[M+K]^+$, indicating a molecular formula of $C_{16}H_{16}O_2$, (calc. 240.1150) formed by conjugation of MeOH (CH_3OH; 32 amu), while the peak at t_R 48.6 exhibited a mass at *m/z* 209 $[M+H]^+$, 231 $[M+Na]^+$, and 247 $[M+K]^+$ corresponding to the molecular formula of $C_{15}H_{12}O$ (calc. 208.0888) of **5**.

Table S1. 1D and 2D NMR data of compounds **1m** and **1**.

	1m[a]				**1**[a]				**1**[b]			
No.	δ_H (*J* in Hz)	δ_C		HMBC	δ_H (*J* in Hz)	δ_C		HMBC	δ_H (*J* in Hz)	δ_C		HMBC
1		131.6	C			131.9	C			131.5	C	
1a	5.85 d (2.0)	102.8	CH_2	1, 2	5.92 s	102.9	CH_2	1, 2	6.01 s	102.5	CH_2	1, 2
2		152.4	C			152.7	C			151.9	C	
3	6.29 s	90.3	CH	1. 2, 5, 6, 1'	6.38 s	90.3	CH	1. 2, 5, 6, 1'	6.48 s	90.4	CH	1, 2, 4, 5
4		154.7	C			154.9	C			154.1	C	
5		117.1	C			115.7	C			115.8	C	
6		142.2	C			142.7	C			142.0	C	
1′		203.4	C			197.6	C			195.7	C	
2′	5.17 dd (7.6, 5.6)	52.4	CH	1', 3', 1", 2", 6"		149.9	C			149.5	C	
3′	4.12 dd (7.6, 10)	73.8	CH_2	1', 2', 1", O<u>C</u>H_3	6.00 d (1.2)	129.8	CH_2	1', 2', 1"	6.04 d (0.8, 16)	130.1	CH_2	1', 2', 1"
	3.61 dd (5.6, 10)			1', 2', 1"	6.06 d (1.2)				6.08 d (1.2, 16)			
1″		123.5	C			126.1	C			125.9	C	
2″		156.8	C			156.1	C			155.5	C	
3″	6.72 m	116.3	CH	2", 5"	6.81 m	116.7	CH	2", 5"	6.88 t (8)	116.9	CH	2", 5"
4″	7.07 t (7.6)	130.4	CH	2", 6"	7.12 m	130.5	CH	2", 6"	7.17 t (8)	130.2	CH	2", 6"
5″	6.73 t (7.6)	120.3	CH	1", 3"	6.81 t (7.6)	120.3	CH	1", 3", 4"	6.83 t (7.6)	120.3	CH	1", 3"
6″	7.02 t (7.6)	129.4	CH	2", 4"	7.11 m	132.1	CH	2', 2", 4"	7.15 m	131.9	CH	2', 2", 4"
	3.36 s	59.0	OCH_3	3'	3.68 s	57.2	OCH_3	4	3.73 s	57.2	OCH_3	4
	3.64 s	57.2	OCH_3	4	3.93 s	60.5	OCH_3	6	3.92 s	60.4	OCH_3	6
	3.76 s	60.4	OCH_3	6					8.05 s		OH	1", 3"

Spectra were recorded at 400 MHz for ^{1}H NMR and 100 MHz for ^{13}C NMR. [a] measured in CD_3OD; [b] measured in acetone-d_6.

Table S2. 1D and 2D NMR data of compounds **3** and **4**.

3					**4**				
No.	δ_H (*J* in Hz)	δ_C		HMBC	No.	δ_H (*J* in Hz)	δ_C		HMBC
2	4.66 dd (9.6, 10.8) 4.51 dd (5.2, 10.8)	71.0	CH_2	3, 4, 8a, 1'	1		131.6	C	
3	4.11 d (5.2)	49.7	CH	2, 4, 1', 2', 6'	1a	6.04 s	102.5	CH_2	1, 2
4		190.3	C		2		152.2	C	
4a		110.4	C		3	6.54 s	90.1	CH	1, 2, 5, 4, 6, 2'
5		144.2	C		4		155.9	C	
6		133.9	C		5		104.9	C	
6a	6.04 dd (0.8, 4.8)	102.9	CH_2	6, 7	6		143.8	C	
7		155.2	C		1'a		155.8	C	
8	6.29 s	93.9	CH	4a, 5, 6, 7, 8a, 4	2'		147.5	C	
8a		161.4	C		3'		119.9	C	
1'		124.1	C		3'a		130.0	C	
2'		156.2	C		4'	7.44 d (7.6)	111.6	CH	1'a, 3'a, 5'
3'	6.89 d (7.6)	116.5	CH	1', 2', 5'	5'	7.27 m	122.9	CH	3'a
4'	7.10 m	129.3	CH	2', 3', 6'	6'	7.23 m	124.6	CH	1'a, 7'
5'	6.79 t (7.6)	120.5	CH	1', 2', 3', 6'	7'	7.80 d (7.3)	121.4	CH	1'a, 6'
6'	7.13 d (7.6)	130.9	CH	3, 2', 4'		3.72 s	57.0	OCH_3	4
	3.92 s	60.8	OCH_3			3.89 s	60.3	OCH_3	6
	8.73 s		OH			4.58 s	56.4	CH_2OH	2' 3', 3'a

[a] Spectra were recorded in acetone-d_6 at 400 MHz for ^{1}H NMR and 100 MHz for ^{13}C NMR.